MARCH 2016

SAN FRANCISCO ESTUARY & WATERSHED SCIENCE

Sponsored by the Delta Science Program and the UC Davis John Muir Institute of the Environment

RESEARCH

Linking Hydrodynamic Complexity to Delta Smelt (*Hypomesus transpacificus*) Distribution in the San Francisco Estuary, USA

Aaron J. Bever,*[1] Michael L. MacWilliams,[1] Bruce Herbold,[2] Larry R. Brown,[3] and Frederick V. Feyrer[3]

Volume 14, Issue 1 | Article 3
doi: *http://dx.doi.org/10.15447/sfews.2016v14iss1art3*

* Corresponding author: *abever@anchorqea.com*

1 Anchor QEA, LLC
San Francisco, CA 94111 USA

2 Consulting Estuarine Ecologist
Oakland, CA 94610 USA

3 U.S. Geological Survey
Sacramento, CA 95819 USA

ABSTRACT

Long-term fish sampling data from the San Francisco Estuary were combined with detailed three-dimensional hydrodynamic modeling to investigate the relationship between historical fish catch and hydrodynamic complexity. Delta Smelt catch data at 45 stations from the Fall Midwater Trawl (FMWT) survey in the vicinity of Suisun Bay were used to develop a quantitative catch-based station index. This index was used to rank stations based on historical Delta Smelt catch. The correlations between historical Delta Smelt catch and 35 quantitative metrics of environmental complexity were evaluated at each station. Eight metrics of environmental conditions were derived from FMWT data and 27 metrics were derived from model predictions at each FMWT station. To relate the station index to conceptual models of Delta Smelt habitat, the metrics were used to predict the station ranking based on the quantified environmental conditions. Salinity, current speed, and turbidity metrics were used to predict the relative ranking of each station for Delta Smelt catch. Including a measure of the current speed at each station improved predictions of the historical ranking for Delta Smelt catch relative to similar predictions made using only salinity and turbidity. Current speed was also found to be a better predictor of historical Delta Smelt catch than water depth. The quantitative approach developed using the FMWT data was validated using the Delta Smelt catch data from the San Francisco Bay Study. Complexity metrics in Suisun Bay were evaluated during 2010 and 2011. This analysis indicated that a key to historical Delta Smelt catch is the overlap of low salinity, low maximum velocity, and low Secchi depth regions. This overlap occurred in Suisun Bay during 2011, and may have contributed to higher Delta Smelt abundance in 2011 than in 2010 when the favorable ranges of the metrics did not overlap in Suisun Bay.

KEY WORDS

hydrodynamic modeling, UnTRIM, low salinity zone, habitat suitability, fall midwater trawl, turbidity, salinity, pelagic organism decline

INTRODUCTION

Peterson (2003) proposed a conceptual model of estuarine habitats as a dynamic aquatic regime overlaying a stationary bathymetric framework that captures much of the physical and habitat complexity of estuaries. River flows and tidal forcing shift the dynamic environment across the stationary base to produce varying environmental conditions for biological organisms. For each species, the overlap of the dynamic and stationary environments affects feeding, predation, survival, growth, and density. For each life stage of each species, there will be different optimal overlaps of stationary and dynamic conditions. In estuaries, salinity is generally the dynamic element that most strongly drives species distribution and composition along with biomass, density, and species richness (e.g., Elliot and Dewailly 1995; Thiel et al. 1995; Marshall and Elliot 1998). The role of temperature, dissolved oxygen, turbidity, and hydrodynamics in structuring fish communities in estuaries varies more from estuary to estuary than the role of salinity (e.g., Elliott and Dewailly 1995; Marshall and Elliott 1998; Barletta et al. 2005). The stationary bathymetric aspects of an estuary can provide both shallow habitats of low velocity and high productivity (e.g., Neves et al. 2013) and deep channels where visual predators are at a disadvantage (e.g., Brabrand and Faafeng 1993).

Moyle et al. (2010) note that "a vast ecological literature documents the significant roles of habitat complexity and variability in promoting abundance, diversity, and persistence in a wide array of ecosystems." For pelagic organisms such as the Delta Smelt (*Hypomesus transpacificus*) of the San Francisco Estuary (estuary), habitat complexity is largely synonymous with hydrodynamic complexity. The food, competitors, and predators of pelagic organisms occur in association with complex hydrodynamic features that vary at all spatial and temporal scales (e.g., at very large scale see Trenkel et al. 2014; at intermediate scales Govoni and Grimes 1992; Bakun 2006; Kai and Marsac 2010; Hood et al 1999; and at smaller scales Thiel et al. 1995; Menendez et al. 2012). Even in laboratory studies, hydrodynamic complexity affects the feeding efficiency of small fish on copepods (Lee et al. 2010).

The principal scientists of the Interagency Ecological Program (a consortium of the nine state and federal agencies doing science in the estuary) identified a primary need to "develop a method of measuring 'hydrodynamic complexity'" (Brown et al. 2014). However, there is currently no established method to quantify hydrodynamic complexity, defined by Brown et al. (2014) as habitat heterogeneity that provides a large array of habitat types for Delta Smelt to use for resting, feeding, and other activities. Brown et al. (2014) note that there remains much uncertainty about the interaction of hydrodynamics with stationary habitat components in Suisun Bay and their combined effects on other dynamic habitat components including turbidity, contaminants, and biota.

The estuary encompasses San Francisco Bay (Central Bay and South Bay), San Pablo Bay, Suisun Bay, and the Sacramento–San Joaquin Delta (Figure 1, inset). The largest sources of freshwater to the estuary are the Sacramento River and the San Joaquin River. The mixing of this freshwater with the saline water from the Pacific Ocean results in an estuary-wide salinity gradient, with salinity varying from more than 30 psu near the Golden Gate to less than 0.1 psu in the Sacramento River. The salinity gradient varies strongly on tidal, seasonal, and annual time scales. The estuary is bathymetrically and hydrodynamically complex; broad shoals are bisected by a network of deeper channels. We focused on the easternmost embayment, Suisun Bay, comprising two relatively flat and shallow sub-embayments: Grizzly Bay and Honker Bay (Figure 1). During fall, the Low Salinity Zone (LSZ), the portion of the estuary with salinity between 0.5 and 6 psu, is often in the vicinity of Suisun Bay (MacWilliams et al. 2015). Although there is a net westward water flow through Suisun Bay resulting from the freshwater outflow from the Delta, the currents within Suisun Bay are primarily driven by the interaction of the semidiurnal tides with a complicated bathymetry (Cheng and Gartner 1984).

Delta Smelt are endemic to the estuary and have declined in abundance, resulting in their listing as a threatened species in 1993 under both the California Endangered Species Act and the federal Endangered Species Act. Efforts to protect Delta Smelt have been contentious and primarily focused on water management and anthropogenic effects on water

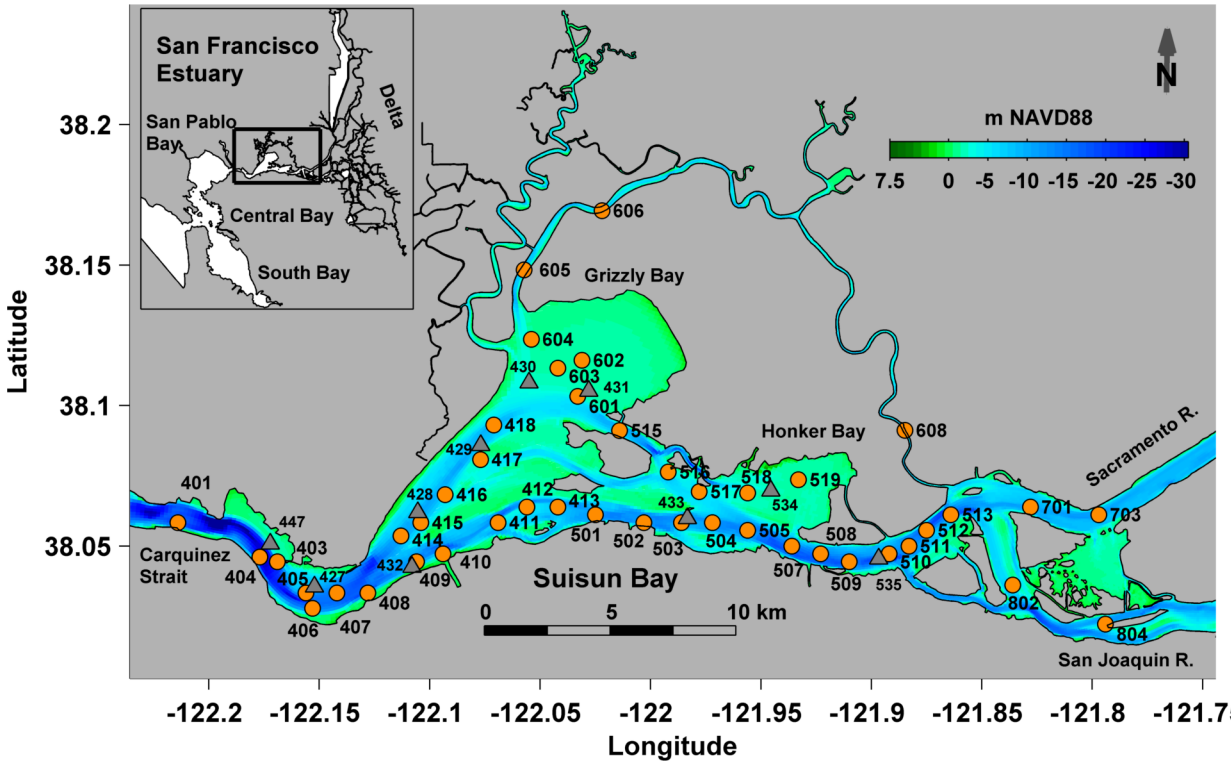

Figure 1 Locations of the FMWT (circles) and Bay Study (triangles) sampling stations in the vicinity of Suisun Bay used in this analysis

quality. Considerable planning has been done to reduce the effect of current water management and to restore the habitats relied upon by Delta Smelt and other species of concern (BDCP 2014; Resources Agency 2012). However, further defining the physical parameters of Delta Smelt habitat is essential for the success of future management actions and habitat restoration efforts (Baxter et al. 2015). To date, descriptions of the physical habitat used by Delta Smelt have relied on concurrent (or nearly so) measures of the salinity, temperature, and turbidity where they have been captured (Moyle et al. 1992; Aasen 1999; Nobriga et al. 2005; Brown and May 2006; Feyrer et al. 2007). Numerical modeling tools now allow estimation of the detailed hydrodynamic conditions throughout the estuary, and analysis of fish catch data with variables that cannot be easily measured in a field setting.

Delta Smelt are caught most often in shallow open water with low salinity, high turbidity, and moderate temperatures (Moyle et al. 1992; Feyrer et al. 2007; Sommer and Mejia 2013). Suisun Bay has historically been a good location for catching Delta Smelt because it has low salinity, high turbidity, and broad shallow areas (Moyle et al. 1992; Merz et al. 2011). Feyrer et al. (2007) found that salinity and turbidity explained about one quarter of the variance in the distribution of Delta Smelt extending from San Francisco Bay through the Delta. Fish catch data shows more frequent Delta Smelt catches in shallow water (Moyle et al. 1992), but it is unknown if Delta Smelt are simply seeking out shallow water or if other environmental conditions lead to more frequent catches in the shallower areas of Suisun Bay.

Recent studies have combined three-dimensional (3–D) numerical modeling and observational data to improve understanding of variation in fish catch in long-term surveys of fish abundances in the estuary (e.g., Kimmerer et al. 2009, 2013). However, these studies have generally evaluated associations using the annual abundance index for the whole estuary as the response variable. This study took a more granular approach, and analyzed the specific environmental conditions at each individual station in the vicinity of Suisun Bay that have historically resulted in Delta Smelt catch. Using a quantitative

http://dx.doi.org/10.15447/sfews.2016v14iss1art3

approach, we evaluated how the interaction of salinity, turbidity, and hydrodynamics affected the likelihood of catching Delta Smelt at a given site. We focused on the physical characteristics of places where Delta Smelt have been caught in accord with the Peterson (2003) conceptual model. This approach avoids the complexities of incorporating predator–prey dynamics (e.g., Walters and Juanes 1993; Essington and Hansson 2004) into habitat descriptions. Our goal was to determine the extent to which the historical fish catch data are correlated with specific quantified environmental conditions, and whether these correlations can be used to improve the monitoring and prediction of fish abundance. This study investigated the spatial distribution of both observed and model-predicted variables that may explain why some stations have historically had both more frequent and higher fall Delta Smelt catches than other stations. This approach builds on earlier work and established hypotheses by investigating the following questions:

1. Which stations have historically had both more frequent and higher fall Delta Smelt catches than other stations?
2. Can quantified metrics based on salinity, turbidity, and hydrodynamics be used to predict the areas favorable for catching a Delta Smelt under specific conditions?
3. How do the environmental variables most correlated to Delta Smelt catch vary interannually?

METHODS

Fall Midwater Trawl Survey

The California Department of Fish and Wildlife's (CDFW) Fall Midwater Trawl (FMWT) began in 1967 and has sampled every year except 1974 and 1979 (Stevens and Miller 1983; Feyrer et al. 2007; CDFW 2014). The FMWT samples at over 100 stations from San Pablo Bay landward into the Sacramento–San Joaquin Delta. Each station is typically sampled once each month from September through December. The mouth of the net is 3.7 m × 3.7 m. The net is hauled obliquely through the water column for 12 minutes, so at shallower stations more time is spent sampling near the surface. The sampling equipment and methods have remained consistent since 1967. Surface conductivity, Secchi depth, water temperature, and (since 2009) turbidity are collected with each tow. Tide, wind, wave, and weather codes are recorded semi-quantitatively. All of the FMWT observed variables were measured from 1967 through 2012 except for turbidity and the distance of each tow. The distance of each tow, as determined by GPS measures, was reported only for 2010 and 2011.

The FMWT was designed to index the year-to-year relative abundance of Striped Bass (*Morone saxatilis*, Stevens and Miller 1983). However, all captured species are identified and measured and the FMWT has become a long-term indicator of population trajectories for several small, pelagic fish, including Delta Smelt (Moyle et al. 1992; Sommer et al. 2007). Although Delta Smelt are caught westward of Suisun Bay in the spring and summer, the majority are caught east of Carquinez Strait (Bennett 2005). To span the extent of the LSZ during the fall period, we used all available survey data from 1967 to 2012 at the 45 FMWT stations in the vicinity of Suisun Bay (Figure 1, Table 1).

San Francisco Bay Study

The San Francisco Bay Study (Bay Study) began monthly otter and midwater trawl sampling in January 1980 (Armor and Herrgesell 1985; Baxter et al. 1999). Bay Study sampling stations span the entire estuary. We used the 10 Bay Study stations in the vicinity of Suisun Bay for the years from 1980 to 2012 (Figure 1). We restricted our analysis to the Bay Study midwater trawl surveys from the months of September through December for comparison with FMWT results. The Bay Study gear and procedures are essentially identical to those of the FMWT.

UnTRIM Bay–Delta Model

UnTRIM is a 3-D hydrodynamic numerical model that solves the Navier–Stokes equations on an unstructured horizontal grid and z-level vertical grid. The governing equations are discretized using a finite difference–finite volume algorithm. The governing equations, numerical discretization, and numerical properties of UnTRIM are described in Casulli (1999),

Table 1 The established geographic station locations of the 45 FMWT stations in the vicinity of Suisun Bay used in this study, the total number of tows conducted between 1967 and 2012, and the calculated catch-based station index, SI_C

Station number	Longitude	Latitude	Number of tows 1967–2012	Station index, SI_C
401	−122.214000	38.058306	212	0.07
403	−122.169000	38.044389	170	0.03
404	−122.176944	38.046111	212	0.07
405	−122.156000	38.033306	231	0.12
406	−122.153000	38.027806	206	0.08
407	−122.142000	38.033306	209	0.12
408	−122.128000	38.033306	175	0.05
409	−122.106000	38.044389	212	0.07
410	−122.094000	38.047194	230	0.10
411	−122.069000	38.058306	212	0.13
412	−122.056000	38.063889	229	0.28
413	−122.042000	38.063917	208	0.23
414	−122.113000	38.053611	234	0.14
415	−122.104000	38.058306	191	0.18
416	−122.093000	38.068306	234	0.21
417	−122.077000	38.080806	191	0.25
418	−122.071000	38.093111	235	0.36
501	−122.025000	38.061111	233	0.30
502	−122.003000	38.058306	214	0.21
503	−121.986000	38.058306	233	0.44
504	−121.972000	38.058306	211	0.27
505	−121.956000	38.055611	230	0.41
507	−121.936000	38.050000	233	0.74
508	−121.923000	38.047194	212	0.57
509	−121.910000	38.044389	229	0.72
510	−121.892000	38.047194	208	0.63
511	−121.883000	38.050000	230	0.80
512	−121.875000	38.055611	198	0.63
513	−121.864000	38.061111	225	0.83
515	−122.014000	38.091111	234	0.65
516	−121.992000	38.076389	208	0.46
517	−121.978000	38.069389	222	0.66
518	−121.956000	38.068889	215	0.83
519	−121.933000	38.073611	235	1.00
601	−122.033000	38.103306	211	0.48
602	−122.031000	38.116111	222	0.81
603	−122.042000	38.113306	213	0.55
604	−122.054000	38.123611	236	0.83
605	−122.057223	38.148296	215	0.80
606	−122.022000	38.169389	235	1.00
608	−121.884847	38.091185	235	0.68
701	−121.828000	38.063889	230	0.89
703	−121.797000	38.061111	234	1.00
802	−121.836000	38.036111	234	0.37
804	−121.794000	38.022194	234	0.46

Casulli and Walters (2000), and Casulli and Zanolli (2002, 2005).

The UnTRIM hydrodynamic model has been implemented in the San Francisco Bay and Sacramento–San Joaquin Delta to simulate tides, inflows and water diversions, water surface elevations, 3–D velocities, and salinity throughout the Bay-Delta system (MacWilliams et al. 2015). The UnTRIM Bay–Delta model spans the entire estuary, from the Pacific Ocean through the Sacramento River and San Joaquin River (Figure 2). Model boundary conditions included tides at the Pacific Ocean, freshwater inflows to San Francisco Bay and the Sacramento–San Joaquin Delta, and water diversions at six locations in the Delta. Nine control structures were implemented in the model, and the Delta Island Consumptive Use (DICU) model (CDWR 1995) was used to represent agricultural diversions and return flows within the Delta (Figure 2). Spatially and temporally varying wind, evaporation, and precipitation were included based on weather stations around San Francisco Bay and the Sacramento–San Joaquin Delta. We used a two-equation turbulence closure model, choosing parameter values of the generic length–scale equation from Warner et al. (2005) to yield the k-ε closure (Umlauf and Burchard 2003). MacWilliams et al. (2015) presented a detailed description of the model boundary conditions and forcing. The UnTRIM Bay–Delta Model has been used previously to examine the location of the 2 psu isohaline in San Francisco Bay (MacWilliams et al. 2015), for studies of fish habitat (Kimmerer et al.

http://dx.doi.org/10.15447/sfews.2016v14iss1art3

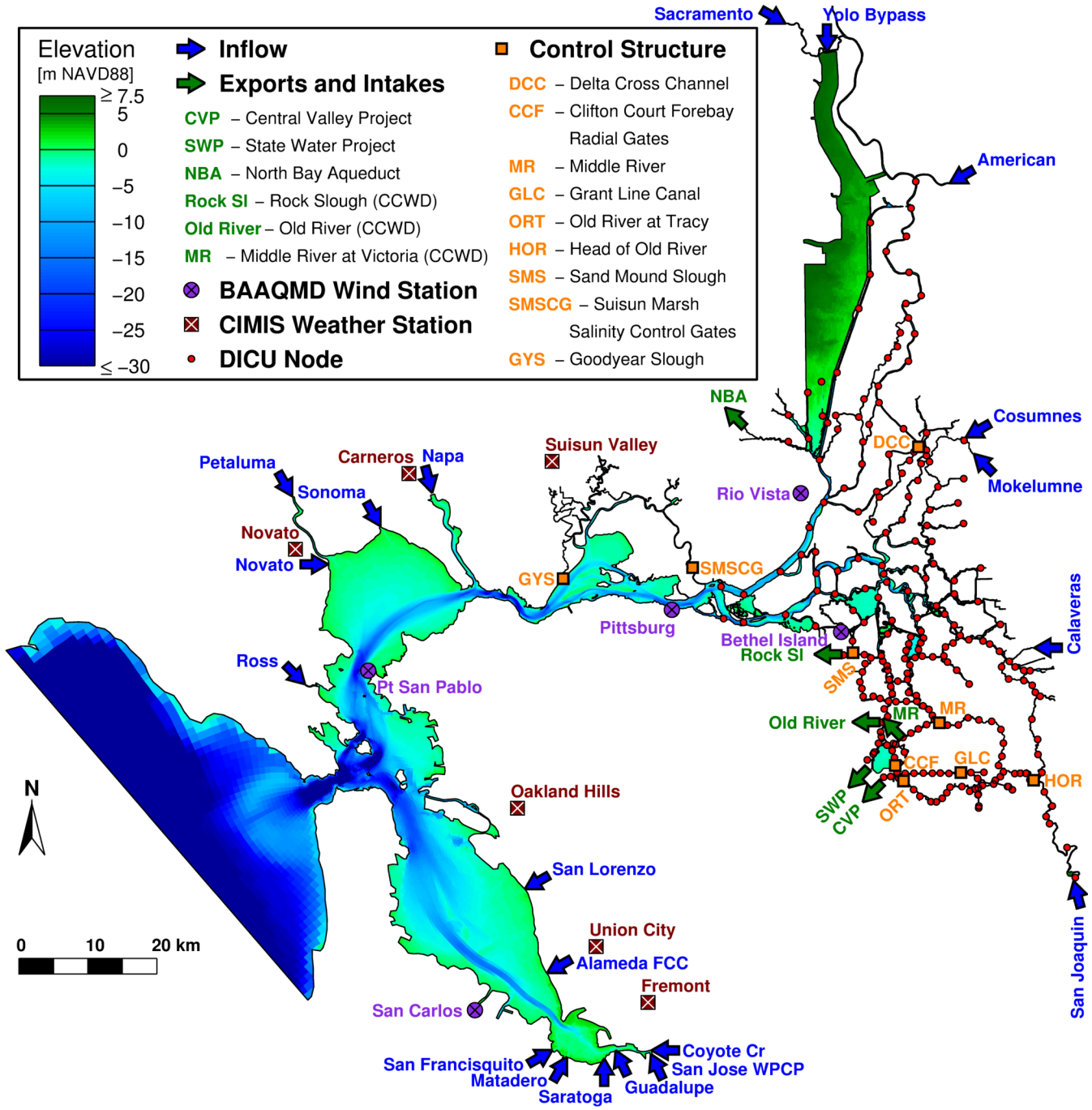

Figure 2 Model domain, bathymetry, and locations of model boundary conditions which include inflows, Delta export facilities and Contra Costa Water District (CCWD) intakes, wind stations from the Bay Area Air Quality Management District (BAAQMD), evaporation and precipitation from the California Irrigation Management System (CIMIS) weather stations, Delta Island Consumptive Use (DICU), and flow control structures.

2009, 2013), to determine the effects on salinity of deepening navigation channels (MacWilliams et al. 2014), to investigate residence time in Clifton Court Forebay in the Delta (MacWilliams and Gross 2013) and to investigate wave- and current-driven sediment transport within the estuary (Bever and MacWilliams 2013). The UnTRIM Bay–Delta model has been extensively validated using water level, salinity, flow, and velocity measurements throughout the entire estuary in numerous previous studies (e.g., MacWilliams et al. 2015).

We simulated 2 years with very different Delta Smelt catches for this study: calendar years 2010 (low catch) and 2011 (high catch). The fall of 2010 had low Delta outflow and high salinity in Suisun Bay; while the fall of 2011 had a relatively uniform and high Delta outflow and lower salinity in Suisun Bay. Our analysis of the model predictions focused on the FMWT sampling period between September 1 and December 31. We validated the spatial and temporal distribution of predicted surface salinity for this study using observations of surface salinity made during each FMWT tow during 2010 and 2011 at the 45 FMWT stations of interest. The model accurately predicted the spatial and temporal variation in surface salinity in Suisun Bay for both 2010 and 2011 (Figure 3).

Calculation of the Historical Delta Smelt Catch Station Index

We used the FMWT Delta Smelt catch data to rank stations based on their relative historical Delta Smelt catch. We developed a quantitative catch-based station index, SI_C. This index takes into account that a single Delta Smelt catch in a tow is currently a success (presence vs. absence) and weights a catch of multiple fish higher than a catch of a single fish. The SI_C was based on the percent of FMWT tows during the 1967–2012 period in which a Delta Smelt was caught, and the total number of Delta Smelt the FMWT caught at each station (Figure 4A). The percent of FMWT tows with a catch and the total number of Delta Smelt caught were then normalized to produce a value between 0 and 1, and a station index based on the historical Delta Smelt catch (SI_C) was calculated as

$$SI_C = \frac{Normalized\ Percent\ Catch + Normalized\ Total\ Catch}{2} \quad (1)$$

The resulting value of SI_C at each station was between 0 and 1, with higher values of SI_C indicating that the station historically had more consistent and/or higher Delta Smelt catches and lower values of SI_C indicating less frequent and/or lower Delta Smelt catches. We then divided the 45 stations used in this

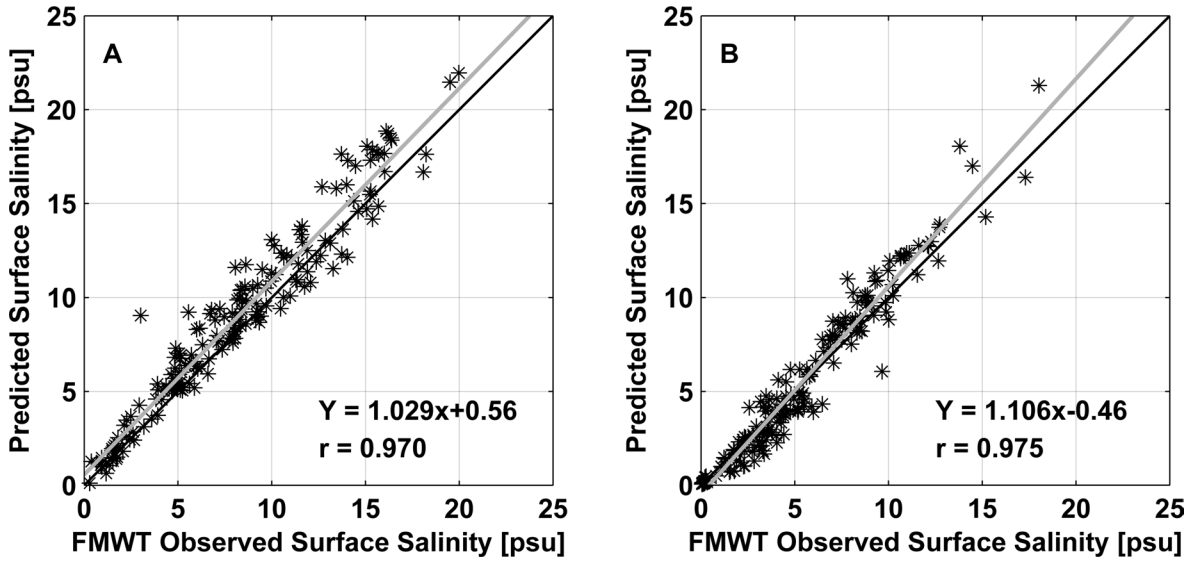

Figure 3 Validation of the model-predicted surface salinity against the FMWT surface salinity for (**A**) 2010 and (**B**) 2011. The black line is the one-to-one line and the grey line is the best-fit line. The equation of the best-fit line and the correlation coefficient are shown in the lower right.

http://dx.doi.org/10.15447/sfews.2016v14iss1art3

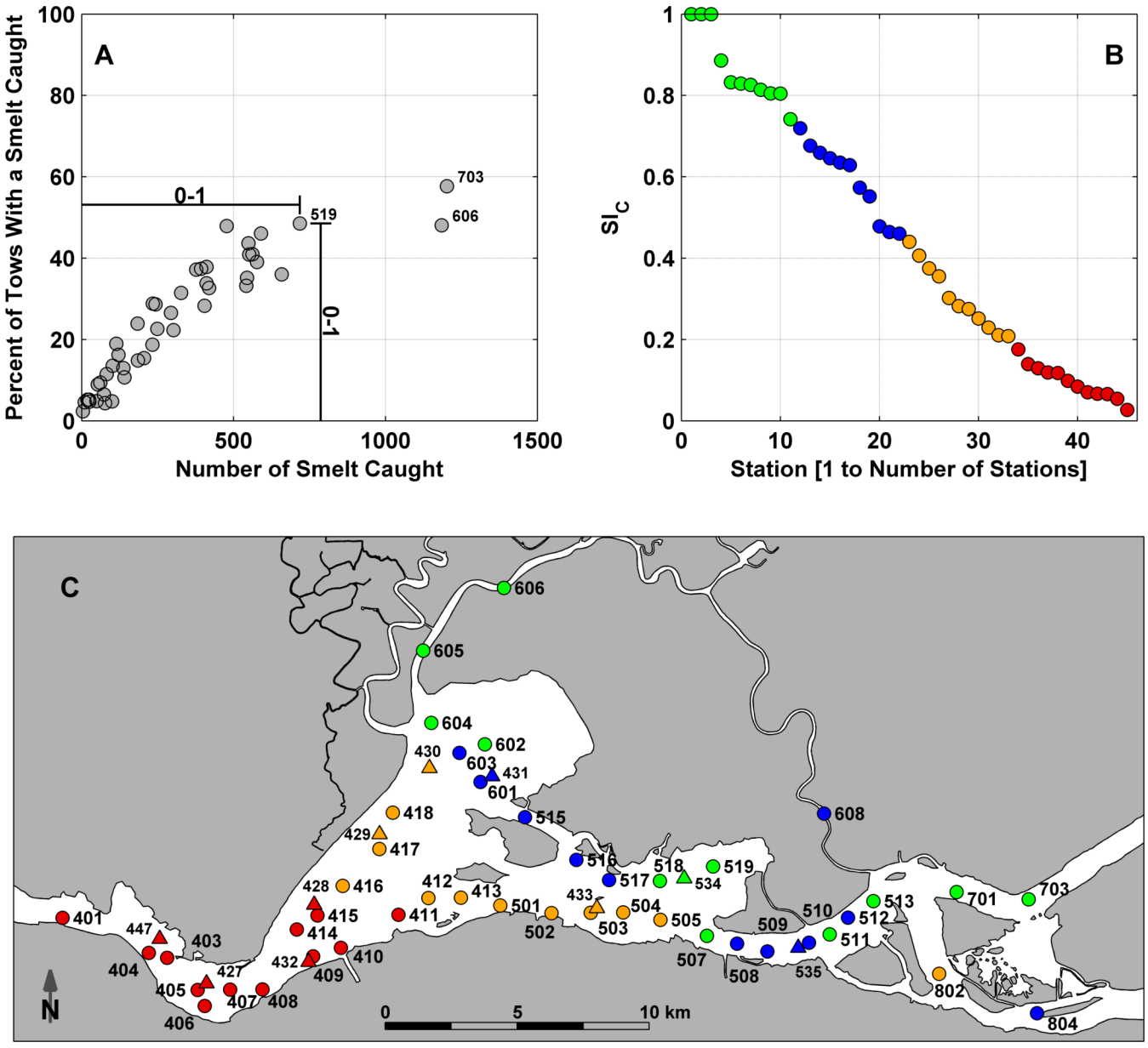

Figure 4 (**A**) Historical FMWT catch data at each station in the vicinity of Suisun Bay; (**B**) the normalized catch-based station index (SI_C) at each of the FMWT stations; and (**C**) the locations of the different SI_C around Suisun Bay labeled with the station number. Station indices are colored based on an equal number of stations in quartile. In (**C**), FMWT stations are shown using circles and Bay Study stations are shown using triangles and slightly smaller numbers.

analysis into four quartiles based on the value of SI_C, with 12 stations included in the lowest quartile and 11 stations in each of the other three quartiles. We identified the quartile of stations with the highest SI_C values as 'good' stations and the lower quartile were identified as 'poor.' We refer to the middle two quartiles collectively as 'medium' stations.

Complexity Metrics

We used 35 environmental variables as "complexity metrics" that quantified either the average or the variability of historical conditions at each station, with each representing a portion of the hydrodynamic complexity surrounding stations in Suisun Bay. We derived eight of these variables from the environmental data collected as part of the FMWT surveys. We calculated the remaining 27 variables from the UnTRIM Bay–Delta model predictions to characterize surface and bottom salinities, surface and bottom velocities, vertical and horizontal gradients in salinity and velocity, and local bathymetry for each FMWT station (Table 2). We chose the 35 complexity metrics *a priori* to the analysis based on published literature that described Delta Smelt distribution and related hypotheses of Delta Smelt in the fall (Moyle et al. 1992; Aasen 1999; Bennett 2005; Feyrer et al. 2007; Sommer and Meija 2013; Brown et al. 2014).

We calculated the complexity metrics derived from the FMWT observation data as the average value at a given station over the full record of historical data. The results from the UnTRIM Bay–Delta model were the model-derived complexity metrics from September through December of 2011, and included maximum or minimum values, mean values, Root-Mean-Square (RMS) values, and standard deviation. Complexity metrics derived from the model predictions included both vertical 1–D metrics based only on the model grid cell that included the established geographic FMWT station location, and 2–D metrics that were based on model predictions within a 550-m diameter circle centered at each station location. Based on the FMWT sampling protocol, 550 m roughly corresponds to the target distance travelled in each tow. Lastly, two modeled complexity metrics were based on the amount of time a variable was within a specific range. These two metrics were the percent of time the salinity at a specific location was within the LSZ—defined here as between 0.5 and 6.0 psu—and the percent of time the depth-averaged salinity at a specific location was less than 6 psu.

Prediction of the Station Index Using Complexity Metrics

We calculated the correlation between each of the complexity metrics and SI_C, and identified the complexity metrics with the highest correlation (either positive or negative) to SI_C (Table 2). A moving-average best-fit line with seven points was used to relate specific values of each complexity metric to individual predictions of the station index. This moving-average approach provided a best-fit line that both followed the data and could be easily used to predict a station index from the quantified complexity metrics. Seven averaging points resulted in lines that followed the data well but did not lead to an excessive number of line segments. The individual station index predictions from the selected metrics were then combined to predict SI_C. We developed a simple equation from a combination of the station indices predicted from the individual salinity, velocity, and turbidity metrics to predict a station index:

$$\begin{aligned} SI_H &= C_1 S + C_2 V && \text{if } T < cutoff \\ SI_H &= (C_1 S + C_2 V) \times C_3 && \text{if } T > cutoff \end{aligned} \quad (2)$$

where SI_H is the predicted station index at a given location based on the environmental conditions; C_1, C_2, and C_3 are coefficients with values between 0 and 1; S is a station index predicted using the best-fit line between a single salinity metric and SI_C; V is a station index predicted using the best-fit line between a single velocity metric and SI_C; and T is a turbidity metric. The equation was based on previous literature indicating that salinity and turbidity strongly influence the location of Delta Smelt (Feyrer et al. 2007, 2011; Sommer and Mejia 2013), but also includes a term based on the hydrodynamics. We developed the form of the equation to allow for different weighting of each of the three complexity metrics. We constrained the values of C such that $C_1 + C_2 = 1.0$, and C_3 was between 0 to 1, to ensure that all values of SI_H were between 0 and 1.

http://dx.doi.org/10.15447/sfews.2016v14iss1art3

Table 2 The complexity metrics calculated from the model predictions and the FMWT data and the correlation of the metric to the catch-based station index, SI_C. 1–D or 2–D indicates whether the metric was calculated based on 1–D values at the station or 2–D values in space around the station, and r is the correlation coefficient between the metric and SI_C. Unless otherwise noted, the metrics are mean values.

Type	Complexity Metric	1–D or 2–D	r	p-Value	Units
Salinity	% of time depth-avg. salinity was less than 6 psu	1–D	0.837	<0.0001	n/a
	% of time depth-avg. salinity was in the LSZ	1–D	0.817	<0.0001	n/a
	Salinity stratification	1–D	−0.813	<0.0001	psu
	Nearbed salinity	1–D	−0.813	<0.0001	psu
	Salinity stratification per meter	1–D	−0.811	<0.0001	psu m^{-1}
	Depth-avg. salinity	1–D	−0.801	<0.0001	psu
	Surface salinity	1–D	−0.768	<0.0001	psu
	Horizontal depth-avg. salinity gradient	2–D	−0.697	<0.0001	psu m^{-1}
Current Speed (CS)	Maximum depth-avg. CS	1–D	−0.533	0.0002	cm s^{-1}
	CS vertical stratification	1–D	−0.467	0.0012	cm s^{-1}
	Depth-avg. RMS CS	1–D	−0.447	0.0021	cm s^{-1}
	Depth-avg. CS (at each station)	1–D	−0.446	0.0022	cm s^{-1}
	Horizontal gradient in nearbed CS	2–D	−0.378	0.0106	cm s^{-1} m^{-1}
	Horizontal gradient in depth-avg. CS	2–D	−0.354	0.0169	cm s^{-1} m^{-1}
	Depth-avg. CS (around each station)	2–D	−0.334	0.0250	cm s^{-1}
	Flood or ebb surface velocity	1–D	0.321	0.0315	cm s^{-1}
	Distance between maximum and minimum depth-avg. CS (used to calculate gradient)	2–D	−0.297	0.0474	m
	Nearbed CS (around each station)	2–D	−0.219	0.1476	cm s^{-1}
	CS vertical stratification per meter	1–D	−0.136	0.3742	cm s^{-1} m^{-1}
	Flood or ebb depth-avg. velocity	1–D	0.129	0.3970	cm s^{-1}
	Distance between maximum and minimum nearbed CS (used to calculate gradient)	2–D	−0.062	0.6842	m
	Flood or ebb bottom velocity	1–D	0.017	0.9102	cm s^{-1}
Bathymetry	Seabed elevation variability (standard deviation)	2–D	−0.510	0.0003	m
	Seabed slope	2–D	−0.461	0.0015	n/a
	Seabed elevation (negative down)	2–D	0.343	0.0209	m NAVD88
	Water depth (time varying with tides, positive down)	1–D	−0.248	0.0999	m
	Distance to shoreline	n/a	−0.037	0.8095	km
FMWT Data	Surface salinity	1–D	−0.789	<0.0001	psu
	Secchi depth	1–D	−0.697	<0.0001	m
	Turbidity	1–D	0.572	<0.0001	NTU
	Distance of tow	n/a	0.350	0.0185	m
	Temperature	1–D	−0.318	0.0334	° C
	Hour of day of sampling	n/a	0.208	0.1700	n/a
	Tide code	n/a	0.174	0.2529	n/a
	Wave code	n/a	−0.157	0.3033	n/a

We first predicted SI_H using only a salinity metric to determine how much of the variability in the station index could be predicted using only salinity. This was accomplished by setting C_1 and C_3 to 1 and C_2 to 0 in Equation 2. We then combined the salinity and the turbidity metrics to predict SI_H to determine if the addition of turbidity improved the accuracy of the predictions. This was accomplished by specifying $C_1 = 1$, $C_2 = 0$ and setting C_3 by minimizing the root-mean-squared difference (RMSD) between SI_C and SI_H. We combined the salinity, turbidity, and velocity metrics to predict SI_H, with C_1, C_2, C_3, and *cutoff* specified to minimize the RMSD between SI_C and SI_H.

Using Equation 2, we computed a value of SI_H at every location within the model domain. We used a weighted average of the turbidity metric based on the distance of each horizontal model grid cell from the two closest FMWT stations to interpolate the value of the observed turbidity metric in each horizontal (2–D) model grid cell. We then used these values of SI_H to produce a 2-D map of the spatial distribution of SI_H, which allows the quantitative analysis developed at the FMWT stations to be applied spatially throughout the study region.

Influence of the Location of Individual Tows on SI_H

We investigated differences between the value of SI_H at the spatial mid-point of each individual tow during 2010 and 2011, and the value of SI_H at the established geographic station location to assess whether the conditions at the exact location of individual tows may have influenced Delta Smelt catch on a tow-by-tow basis in 2010 and 2011. Differences between the conditions at the midpoint of individual tows and the conditions at the established geographic station location could cause tows to be in environmentally different areas than the established geographic station location. Such differences would increase variability in predictions of Delta Smelt catch relative to the variability based on the average conditions at the geographic station location, since the conditions sampled in each tow would vary depending on where the tow occurred relative to the established geographic station location.

Validation of Approach Using Bay Study Data

Using Equation 1, we calculated SI_C from the Bay Study midwater trawl catch data for Delta Smelt at each of the 10 Bay Study stations. We also calculated SI_H for each Bay Study station with Equation 2, using the same three metrics, coefficients, and turbidity cutoff as determined from the FMWT data set. We then compared the values of SI_H and SI_C based on the Bay Study data to determine if the coefficients fit using the FMWT data also applied to the Bay Study data.

Analysis of Interannual Variability

We examined interannual variability in the individual complexity metrics and in SI_H relative to average historical conditions by comparing the values from fall 2010, when the outflow from the Delta was low, and fall 2011, when the outflow was higher and salinities were lower. We compared the different spatial distributions of SI_H in Suisun Bay between these 2 years to provide insight into how different environmental conditions in Suisun Bay during 2 different years influenced the likelihood of Delta Smelt catch.

RESULTS

Calculation of the Historical Delta Smelt Catch Station Index

The relationship between the percent of historical tows in which a Delta Smelt was caught and the total number of Delta Smelt caught showed a consistent positive trend (Figure 4A). The trend shown in Figure 4A was generally reproduced when we examined the FMWT data by decade from 1967 through 2012; however, the scatter about the trend increased when the analysis time period was shortened. We normalized the percent of FMWT tows with a catch and the total number of Delta Smelt caught at each station based on the values calculated for station 519 (Figure 4A). FMWT Stations 703 and 606 were not included in the normalization to prevent skewing of the normalization based on the high number of Delta Smelt caught at these two stations (Figure 4A). We gave FMWT Stations 703 and 606 a SI_C value of 1.0 (the same value calculated for Station 519). The distribution of values of SI_C between the four quartiles is shown in Figure 4B. The

http://dx.doi.org/10.15447/sfews.2016v14iss1art3

value of SI_C showed a general west-to-east increase in the catch-based station index, yet also showed substantial small-scale spatial variability within the larger west-to-east trend (Figure 4C). For example, neither the clusters of 'good' and 'medium' stations around the bathymetric gradients near the western side of Grizzly Bay (601 through 604) and Honker Bay (504, 505, 517, and 518), nor the distribution in SI_C between the stations on the Sacramento River and the San Joaquin River (701, 703, 801, and 802) can be explained based on the west-to-east salinity gradient (Figure 4C).

Complexity Metrics

The metrics based on salinity, both from the 2011 model predictions and the FMWT survey data, were consistently the most highly correlated with SI_C (Figure 5, Table 2), with the observed and predicted surface salinity metrics very similar (Figure 5). Since the salinity metrics were highly correlated to each other, only the salinity metric with the highest correlation to SI_C was selected for further analysis. Of the salinity metrics, the highest correlation to SI_C was for the percent of the time that the salinity at a station was less than 6 psu ($r = 0.837$). The highest correlation for a metric not based on salinity was for Secchi depth from the observed FMWT data ($r = -0.697$). We also selected the water velocity metric with the highest correlation to SI_C for further analysis. Of the 14 metrics based on water velocity, the metric that characterized the maximum depth-averaged current speed at each station was the most highly correlated with SI_C ($r = -0.533$). Seabed elevation, water depth, and distance to shoreline were all less correlated to SI_C than the salinity, Secchi depth, and maximum depth-averaged current speed (Table 2). The correlations with the catch-based

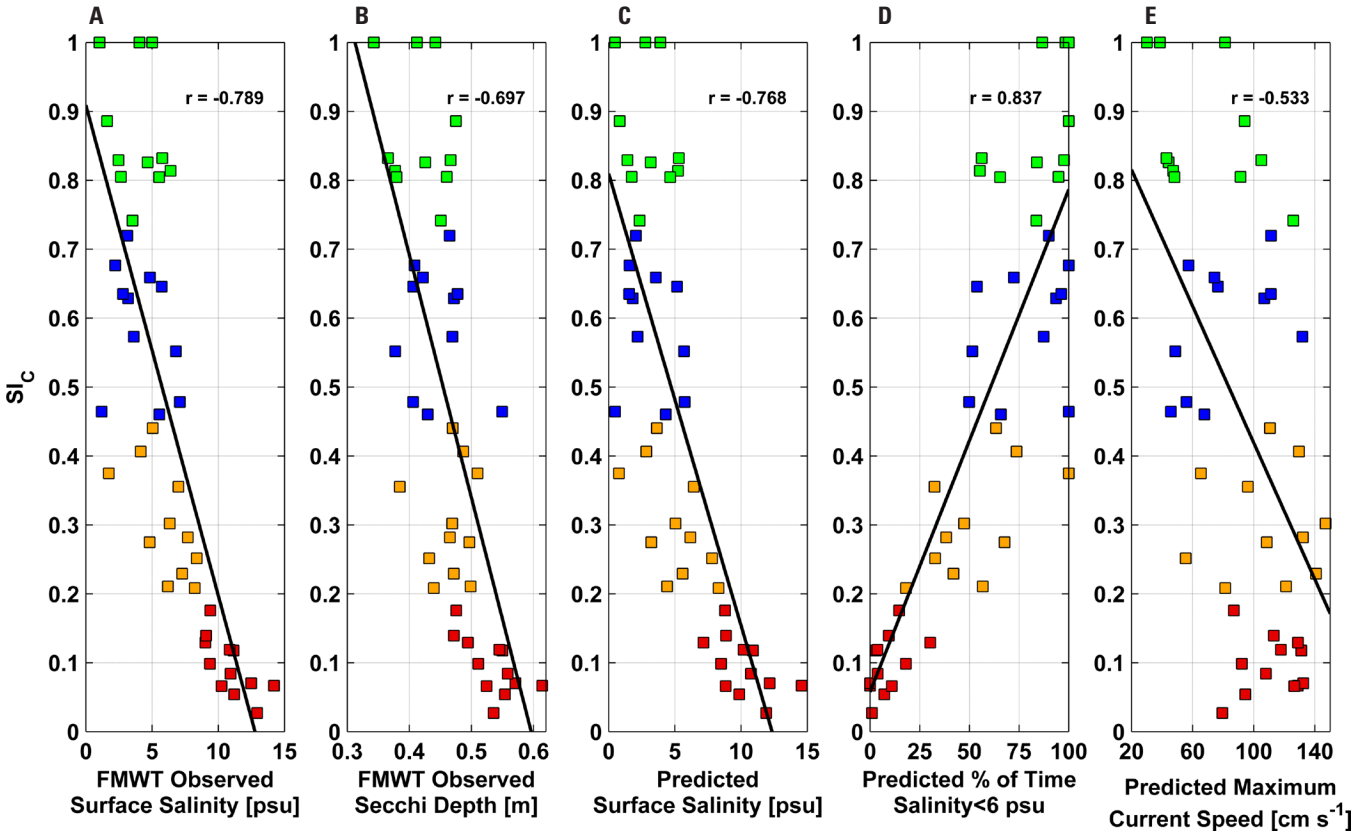

Figure 5 The correlation of select complexity metrics to the catch-based station index, SI_C, for (**A**) surface salinity; (**B**) Secchi depth from the historical FMWT data and the model predicted; (**C**) surface salinity averaged over the fall of 2011; (**D**) percent of the fall when salinity was less than 6 psu; and (**E**) the maximum depth-averaged current speed at each station over the fall of 2011. Each square represents the value of SI_C and the complexity metric for a single station in the vicinity of Suisun Bay. Stations are color coded based on Figure 4B.

station index, SI_C, suggested that the 'poor' stations (colored red) were generally characterized by higher salinity, faster current speeds, and higher Secchi depth (Figure 5). Conversely, 'good' stations (colored green) had lower salinity, slower current speed, and lower Secchi depth.

Prediction of the Station Index Using Complexity Metrics

The percent of time the depth-averaged salinity at a station was less than 6 psu, the maximum depth-averaged current speed at a station, and the Secchi depth at each station had the highest correlation with SI_C, while still representing fundamentally different characteristics of each station, namely the salinity, hydrodynamics, and turbidity. We calculated the percent of time the depth-averaged salinity was less than 6 psu, and the maximum depth-averaged current speed metrics using the 2011 model predictions; we calculated the Secchi depth metric using the FMWT data. There was some correlation between the metrics themselves. The correlation coefficient between the percent of time the depth-averaged salinity at a station was less than 6 psu and the Secchi depth was −0.44. The correlation coefficient between the percent of time the depth-averaged salinity at a station was less than 6 psu and the maximum depth-averaged current speed was −0.34. The correlation coefficient between the Secchi depth and maximum depth-averaged current speed was 0.60.

In Equation 2, we used the percent of time the salinity at a station was less than 6 psu as the salinity variable (to predict S) and the maximum depth-averaged current speed at a station as the water velocity variable (to predict V). We used moving-average best-fit lines to relate the salinity (Figure 6A) and velocity (Figure 6B) metrics to SI_C. We used the Secchi depth metric as the turbidity threshold variable (T) in Equation 2, and determined the Secchi depth threshold for negatively affecting the predictions of the SI_C to be 0.5 m (Figure 6C). When Secchi depth was included as a continuous variable in Equation 2 in the same manner as salinity and velocity, the range of values of SI_H was not well predicted in either eastern Suisun Bay or the confluence region, whereas applying turbidity as a threshold variable in Equation 2 resulted in better predictions of SI_H in these regions. We did not use direct turbidity measurements to predict SI_C because of the very short history of measurement in the FMWT and because the correlation between turbidity and SI_C was lower than the correlation between Secchi depth and SI_C.

As expected, salinity was highly predictive of SI_C, but including velocity and Secchi depth metrics further improved the predictions of SI_C compared with using only salinity. Predicting SI_H using only the salinity metric produced a slope to the best-fit line near one (0.98), indicating that the general west-to-east trend in the historical catch-based station index (SI_C) was captured using only salinity (Figure 7A, Table 3). However, there was considerable scatter about the best-fit line. We then combined the salinity and the Secchi depth to predict SI_H to determine how the addition of the Secchi depth modified the predictions (Figure 7B). The addition of the Secchi depth threshold metric greatly improved the prediction of SI_H at Stations 802 and 804 in the lower San Joaquin River, and also reduced the predicted SI_H for the stations around Carquinez Strait, where SI_C is generally less than about 0.1 (Figure 7B). Finally, we used the salinity, Secchi depth, and velocity metrics to predict SI_H (Figure 7C, Table 3). The addition of the velocity metric further reduced the scatter about

Table 3 Best-fit line statistics between SI_C and SI_H, coefficients used in Equation 2, and the RMS difference between SI_C and SI_H

Metrics used	Best-fit line statistics				Coefficients for Equation 2			RMS difference between SI_C and SI_H
	r	p-Value	Slope	Intercept	C_1	C_2	C_3	
Salinity	0.81	<0.001	0.98	0.04	1.00	0.00	1.00	0.220
Salinity and Secchi	0.86	<0.001	1.02	-0.01	1.00	0.00	0.43	0.183
Salinity, Secchi, and velocity	0.94	<0.001	0.93	0.02	0.67	0.33	0.42	0.106

http://dx.doi.org/10.15447/sfews.2016v14iss1art3

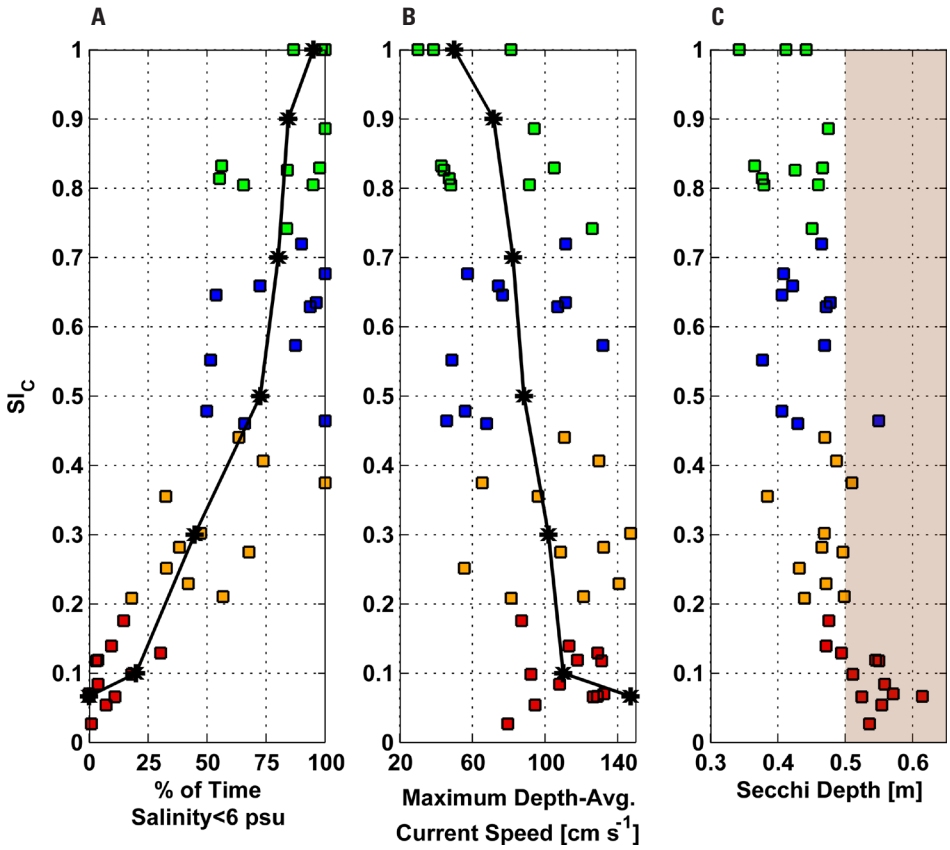

Figure 6 Moving-average best-fit lines relating the complexity metrics to the catch-based station index, SI_C, for (**A**) the predicted percent of time during the fall the depth-averaged salinity was less than 6 psu; (**B**) the predicted maximum depth-averaged current speed; and (**C**) the Secchi depth from the FMWT data. Each square represents the SI_C and complexity metric for a single station. Stations are color coded based on Figure 4B. Shading in (**C**) highlights Secchi depths greater than the 0.5 m threshold.

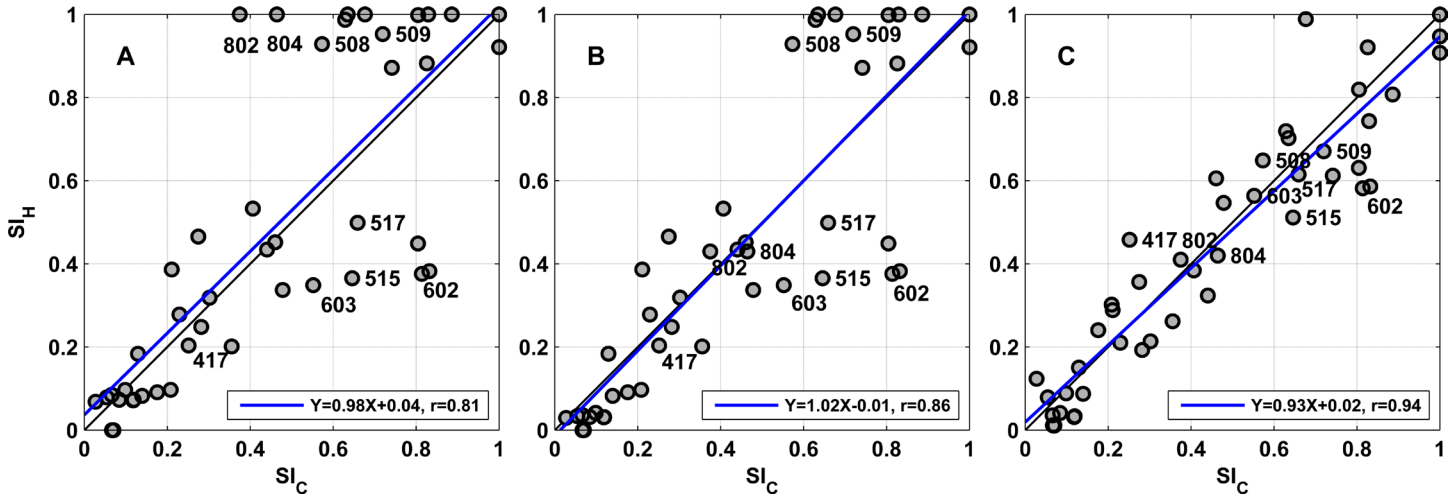

Figure 7 The catch-based station index from the FMWT Delta Smelt catch data, SI_C, and predicted using Equation 2 (SI_H) for each station in the vicinity of Suisun Bay: (**A**) is SI_H based solely on the percent of time the depth-averaged salinity was less than 6 psu; (**B**) also includes the Secchi depth threshold at each station; and (**C**) is SI_H based on the percent of time the depth-averaged salinity was less than 6 psu, the maximum depth-averaged current speed, and the Secchi depth threshold at each station. The black lines show a one-to-one line and the blue lines are the least-squares best-fit lines. Stations identified in the text are labeled.

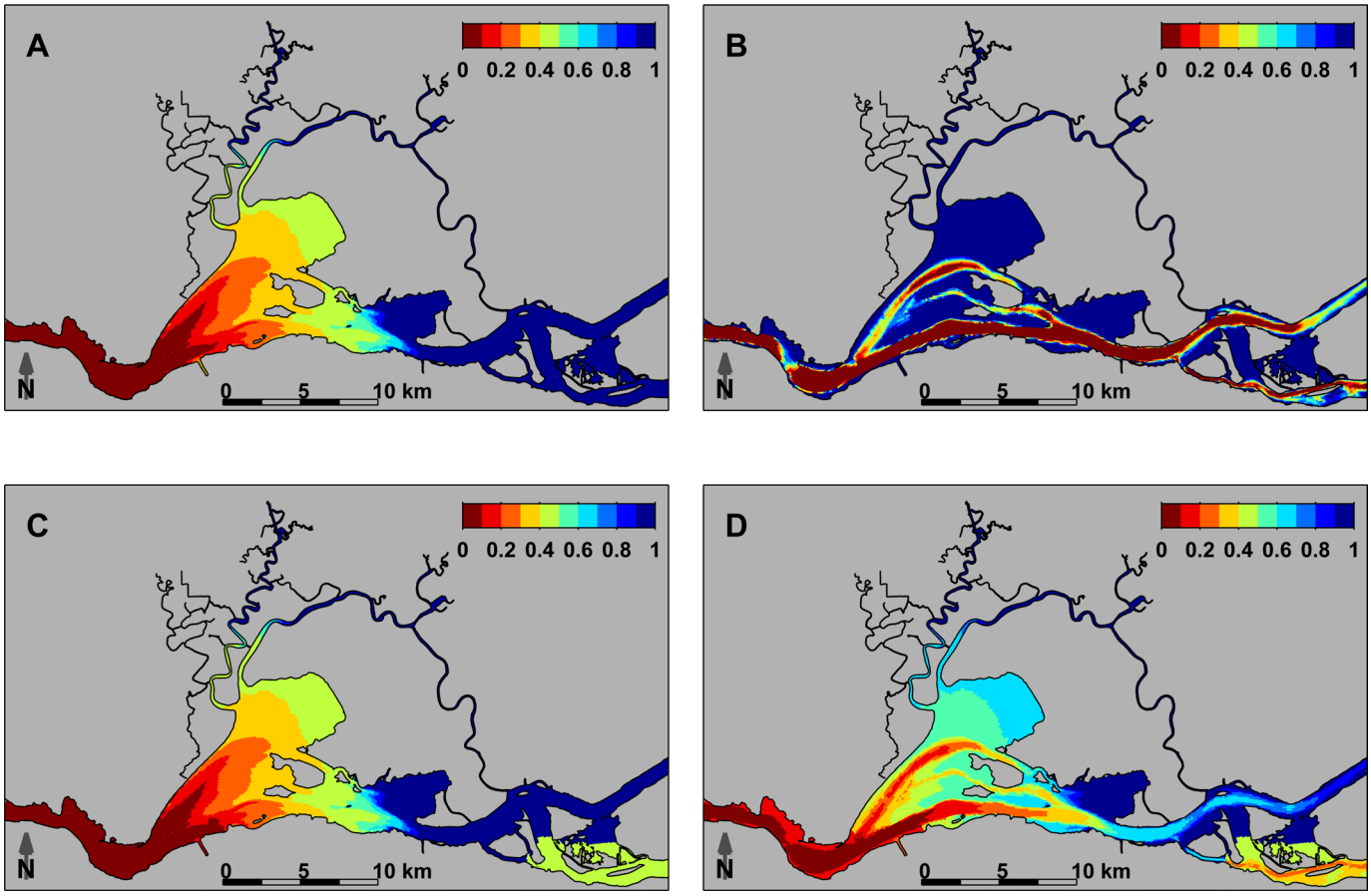

Figure 8 Two-dimensional maps of the station index (SI_H) based on (**A**) the predicted percent of time the depth-averaged salinity was less than 6 psu; (**B**) the maximum depth-averaged current speed; (**C**) percent of time the depth-averaged salinity was less than 6 psu and the Secchi depth threshold; and (**D**) the salinity and velocity metrics with the Secchi depth threshold.

the best-fit line, and improved the prediction of SI_H at many stations that are located in or near the main channels in Suisun Bay, for example stations 508, 509, 515, 517, 602, and 603 (Figure 7C). The salinity metric was weighted about twice as strongly in Equation 2 as the velocity metric (C_1 = 0.67 and C_2 = 0.33).

Using Equation 2 and the coefficients developed above (Table 3), we predicted the value of SI_H at every model grid cell in Suisun Bay. A 2–D map of SI_H at each grid cell based solely on salinity (equivalent to Figure 7A) showed the west-to-east influence of decreasing salinity on SI_H (Figure 8A). A similar map of SI_H at each grid cell based solely on the maximum depth-averaged current speed showed the negative influence of higher maximum depth-averaged current speed on SI_H in the channels (Figure 8B). Including both the salinity metric and the Secchi depth metric (equivalent to Figure 7B) reduced SI_H in Carquinez Strait and in the San Joaquin portion of the confluence region of the Sacramento and San Joaquin rivers (Figure 8C). Combining all three complexity metrics (equivalent to Figure 7C) produced a map of the spatial distribution of SI_H with increasing index from west to east; lower SI_H in the main channels and in the San Joaquin River from the influence of velocity and turbidity, respectively, and higher values of SI_H in Grizzly Bay than were predicted solely using salinity (Figure 8D).

Influence of the Location of Individual Tows on SI_H

The approach used to correlate the catch-based station index (SI_C) to the hydrodynamic-based

http://dx.doi.org/10.15447/sfews.2016v14iss1art3

station index (SI_H) inherently assumed that the tows occurred exactly at the established geographic station location (Table 1). However, the information available on the exact start and end positions of the tows during 2010 and 2011 indicates that the tows did not always take place within the 550-m diameter circle assumed at each station (Figure 9). It is not known whether the FMWT tow locations in 2010 and 2011 are representative of the FMWT tow locations over the entire historical record between 1967 and 2012.

For the 45 stations used in this analysis, the difference between the value of SI_H at the established geographic station location and at the midpoint of the eight tows during 2010 and 2011 was within the range of ±0.2 SI_H, with about 80% of the differences between −0.05 and 0.05 SI_H and about 95% of the differences between −0.1 and 0.1 SI_H. This suggests that, on average, it is not likely that the difference in locations meaningfully affected the prediction of SI_H. However, at some FMWT stations the difference between the established geographic station location and the location of individual tows did noticeably influence the prediction of SI_H in a meaningful way. For example, the prediction of SI_H for Station 417 would be slightly lower if the location used to predict the station index was moved from the established geographic station location to the mid-point of the 2010 and 2011 tows (Figure 9, black), largely because 2010 and 2011 tows typically occurred closer to the main channel, where velocities tended to be higher than at the established geographic station location in a shallower location adjacent to the channel. A lower predicted value for SI_H at Station 417 would result in a prediction closer to the value of SI_C at this station (Figure 7C). This suggests that some of the differences between SI_C and SI_H—and thus some of the scatter on Figure 7C—may be caused by tows not always occurring at the established geographic station locations.

The predictions of SI_H were less sensitive to the actual locations of the tows relative to the established geographic station location for stations in regions of consistent salinity and hydrodynamic conditions where the value of SI_H is less spatially variable. For example, at Stations 602 and 603 (Figure 9, yellow and dark purple, respectively), the locations of the tows in 2010 and 2011 were rarely near the established geographic FMWT station location; however, the predicted value of SI_H for stations 602 and 603 was always between 0.5 and 0.6 at both the established geographic station location and at the mid-point of all of the tows, indicating that, at these two stations, uncertainty in the exact position of the tow would not strongly affect the predicted value of SI_H.

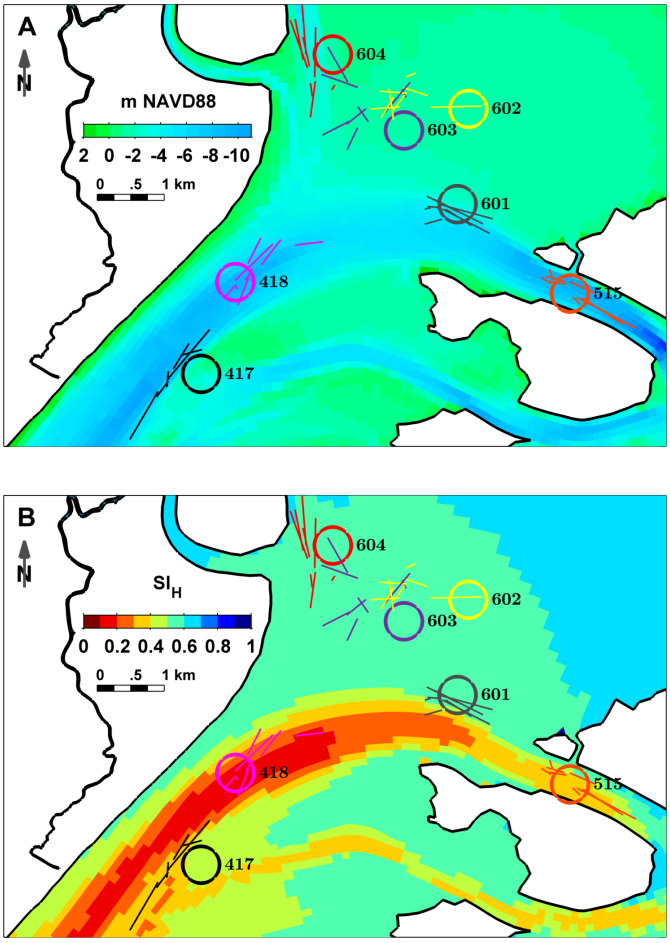

Figure 9 (**A**) Bathymetry and (**B**) SI_H with the individual tow locations from 2010 and 2011 for FMWT stations 417, 418, 515, 601, 602, 603 and 604. Circles represent a 550-m diameter circle around the established geographic station location. Lines show individual tow tracks (based on the start and end locations) and are color coded to match the corresponding station locations.

Validation of Approach Using Bay Study Data

When the value of SI_C was calculated using the historical Bay Study catch data and Equation 1, the value of SI_C at each Bay Study station in the vicinity of Suisun Bay (Figure 4C, triangles) was similar to

that predicted using the FMWT survey catch data at nearby FMWT stations (Figure 4C, circles). This suggests that as long as the data set is of sufficient duration and scope, this method of determining SI_C is robust.

We compared the SI_C calculated from the Bay Study Delta Smelt catch data to the value of SI_H calculated at each Bay Study station using the same three complexity metrics and the same three coefficients for Equation 2 as we used in the FMWT analysis. The value of SI_H predicted at the 10 Bay Study stations was similar to the value of SI_C derived from the Bay Study catch data (Figure 10). The correlation between SI_H and SI_C using the Bay Study data (r = 0.94) was the same as the correlation between SI_H and SI_C using the FMWT data (Figure 7C, r = 0.94) and the slope of the best-fit line was also nearly 1.0. The validation of SI_H using an entirely different data set than was used to develop Equation 2 indicates that the method of predicting a station index from complexity metrics is likely broadly applicable throughout Suisun Bay.

Analysis of Interannual Variability

The model predictions and the FMWT data at each station showed that although salinity and turbidity metrics varied greatly from year to year, water velocity metrics were largely unchanged. The surface salinity in 2011 was lower than in 2010, and the percent of time the depth-averaged salinity was less than 6 psu was higher in 2011 (Figures 11A and 11B). In contrast to the salinity metrics, the metrics based on velocity were nearly identical for 2010 and 2011 (Figures 11C through 11F).

Using 2–D maps to visualize the three complexity metrics included in Equation 2 highlights the different spatial patterns between 2010 and 2011. The percent of the time the salinity was less than 6 psu (Figures 12A and 12B) and the average observed Secchi depth from the four FMWT surveys in each year (Figures 12C and 12D) varied significantly between 2010 and 2011, although the maximum depth-averaged current speeds were nearly the same (Figures 12E and 12F). Figure 12 shows that the drier year (2010) had higher salinities and Secchi depths than the wetter year (2011). The interannual variability in salinity and Secchi depth resulted in markedly different spatial distributions of SI_H in Suisun Bay between 2010 and 2011 (Figure 13).

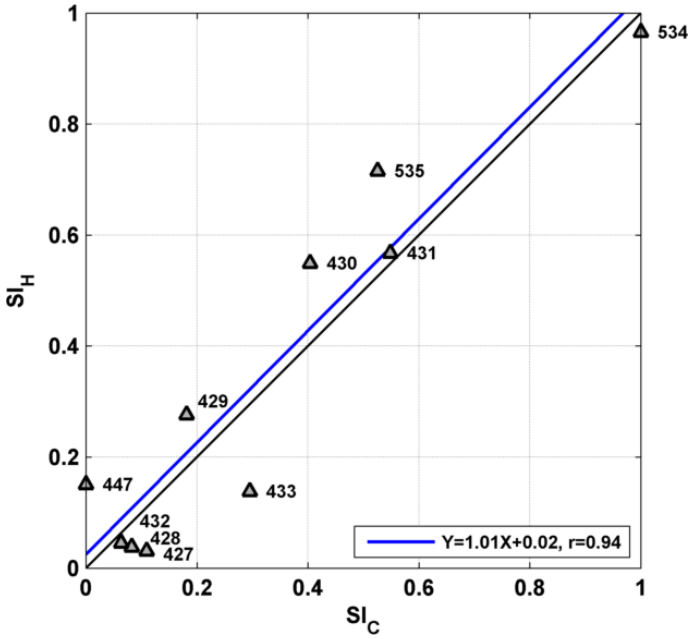

Figure 10 The catch-based station index calculated from the Bay Study data (SI_C) and predicted by Equation 2 (SI_H) for each Bay Study station in the vicinity of Suisun Bay. The black line shows a one-to-one line and the blue line is the least-squares best-fit line.

DISCUSSION

Prediction of the Station Index Using Complexity Metrics

The current literature on Delta Smelt in the San Francisco Estuary does not contain a quantified tabular metric for the ranking of sampling stations based on their historical catch of Delta Smelt. A simple metric was put forth based on both the number of fish caught and the percent of tows with a catch (presence vs. absence) that can be used to quantify the relative ranking of a station for Delta Smelt catch (Table 1). The same general ranking of stations developed using the entire FMWT catch data set could be reproduced even when the data set was evaluated by decade. This indicates that the relative station ranking is not highly sensitive to the decline in Delta Smelt abundance through time. The consistency of the general ranking of stations based on SI_C indicates that the stations that have

http://dx.doi.org/10.15447/sfews.2016v14iss1art3

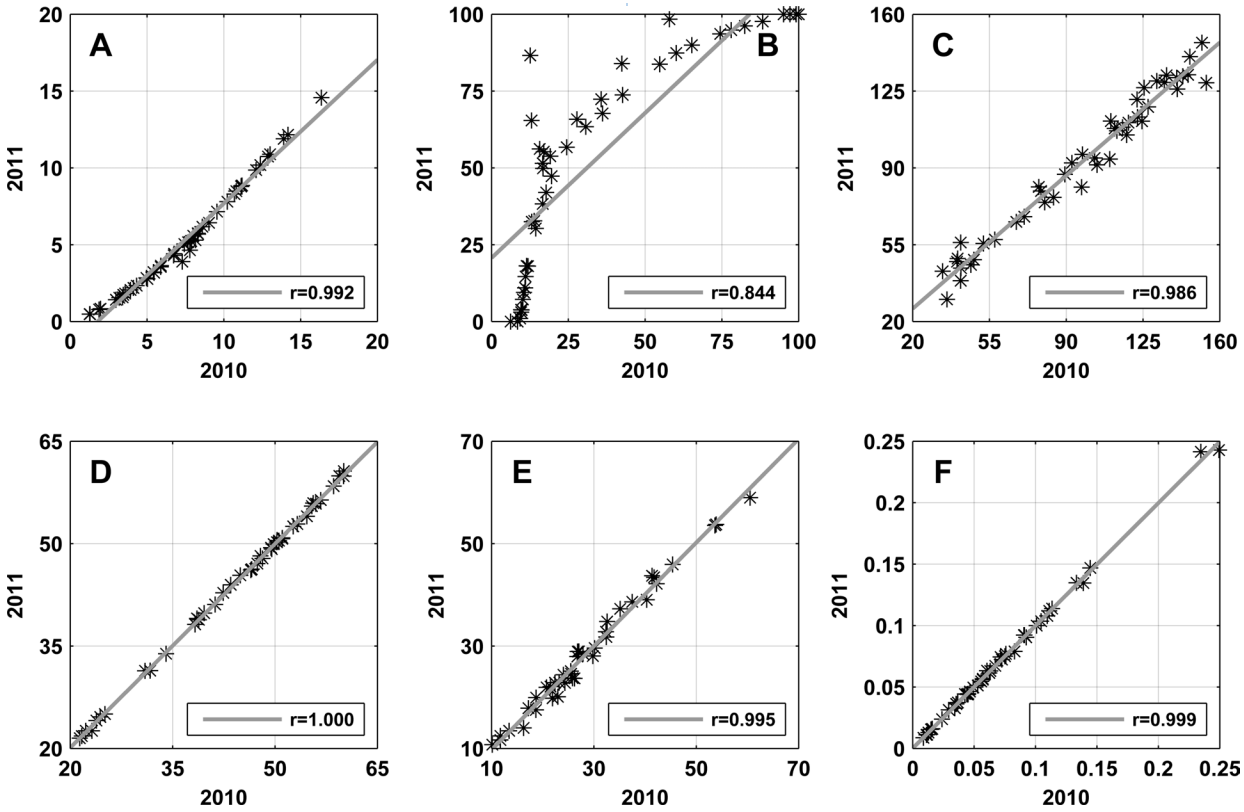

Figure 11 Comparison of salinity and velocity metrics calculated from the numerical model predictions at each station in the vicinity of Suisun Bay for the fall of years 2010 and 2011. The complexity metrics are the (**A**) fall-averaged surface salinity, (**B**) percent of the fall that the depth-averaged salinity was less than 6 psu, (**C**) maximum depth-averaged current speed over the fall, (**D**) fall-averaged depth-averaged current speed, (**E**) fall-averaged vertical stratification in the current speed and (**F**) fall-averaged horizontal gradient in the depth-averaged current speed at each of the stations in the vicinity of Suisun Bay.

historically been good for Delta Smelt catch have remained good throughout the period of declining Delta Smelt abundance.

To relate the quantified SI_C values to current understandings of Delta Smelt based on environmental conditions, we predicted the ranking of stations (SI_H) using salinity, velocity, and turbidity metrics. We inferred the estuarine salinity gradient to be the cause of the general west-to-east increase in SI_C (Figure 4C) because the salinity metric was weighted twice as strongly as the velocity metric in the SI_H predictions (Equation 2, Table 3). This is consistent with the consensus that Delta Smelt prefer regions of salinity less than 6 psu (Sommer and Mejia 2013). Our analysis indicated that in Carquinez Strait and the lower San Joaquin River the Secchi depth has historically been higher than the 0.5-m threshold used to calculate SI_H, indicating lower turbidity and poorer conditions for Delta Smelt than would be predicted based only on salinity. This is consistent with other findings that show Delta Smelt broadly prefer higher turbidity (Feyrer et al. 2007; Sommer and Mejia 2013) and that the lower San Joaquin River is generally less turbid and has a lower Delta Smelt catch than the Sacramento River during nearly co-occurring sampling (Bennett and Burau 2015).

Adding the velocity metric improved the prediction of SI_H at many of the stations that were not well-predicted based solely on the salinity and Secchi depth (Figure 7). This indicates that current speeds were also a useful metric for predicting the historical ranking of a station for Delta Smelt catch. The negative correlation between maximum depth-averaged current speed and SI_C indicated that

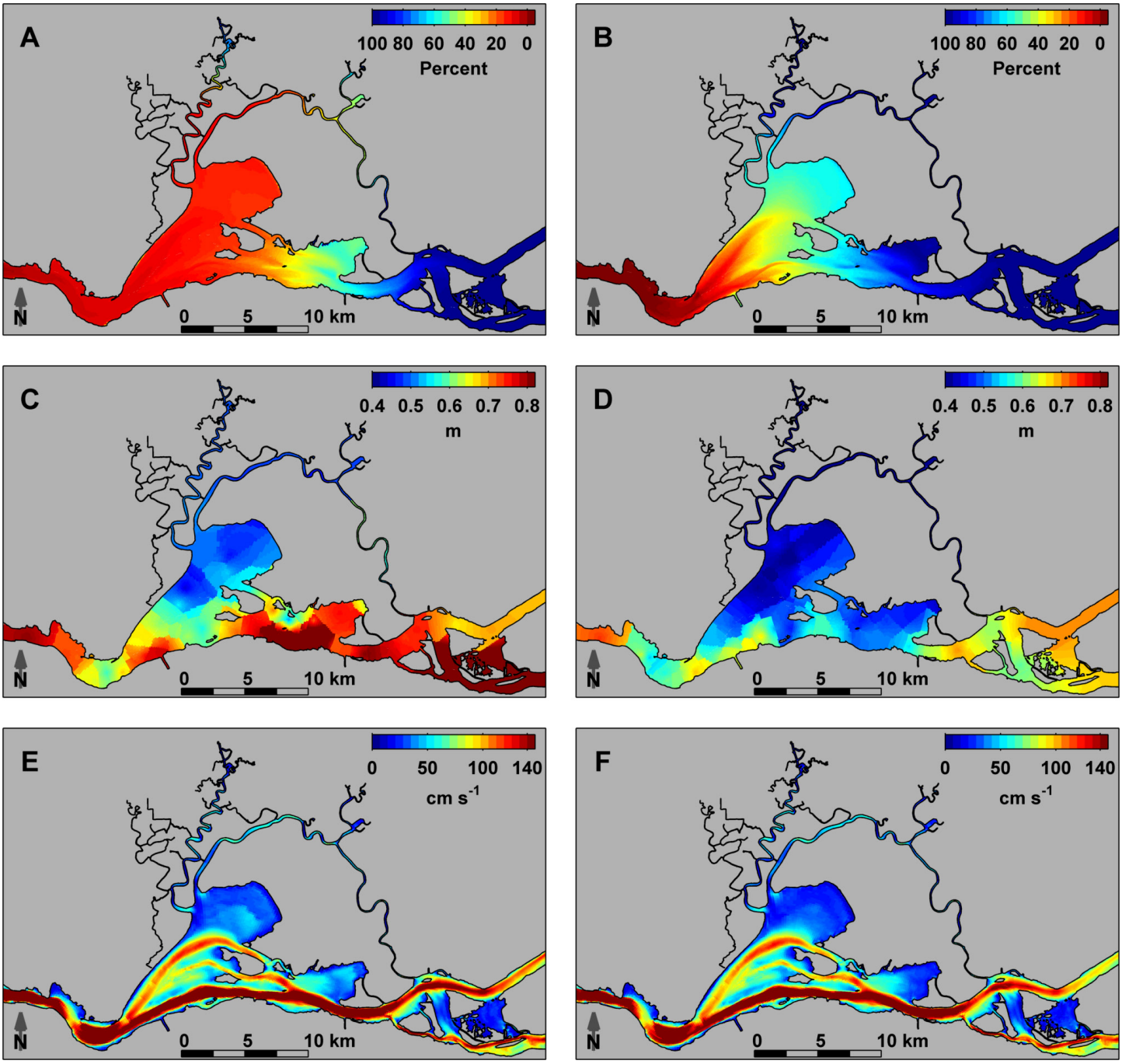

Figure 12 Complexity metrics calculated for the fall of 2010 (left column: **A**, **C**, **E**) and 2011 (right column: **B**, **D**. **F**). The complexity metrics are (**A**, **B**) the percent of the time during fall the depth-averaged salinity was less than 6 psu, (**C**, **D**) the average of the FMWT Secchi depths interpolated onto the model grid, and (**E**, **F**) the maximum depth-averaged current speed during the fall.

http://dx.doi.org/10.15447/sfews.2016v14iss1art3

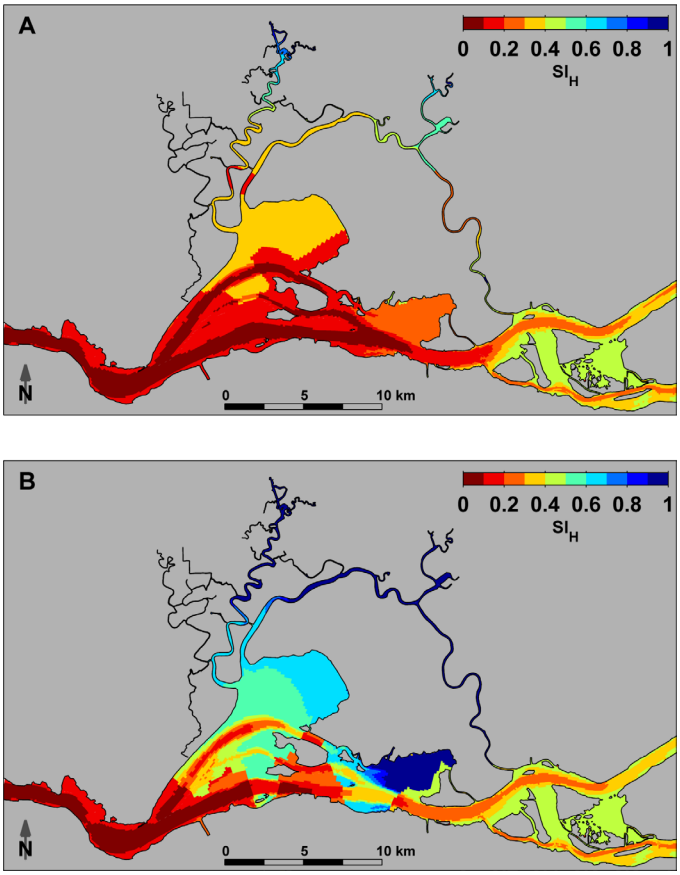

Figure 13 Spatial distribution of SI_H using the complexity metrics from Figure 12 for (**A**) 2010 and (**B**) 2011

Delta Smelt have historically been less likely to be caught in places that experience high current speeds. However, it is possible that the maximum depth-averaged current speed was not necessarily the mechanistic driver behind the spatial variation in SI_C. Since high maximum depth-averaged current speeds typically occur in channels, selection against these areas may indicate fish movement between the channels and shoals (e.g., Aasen 1999; Bennett and Burau 2015), the vertical movement of Delta Smelt in the water column (e.g., Feyrer et al. 2013), or potential differences in sampling gear efficiency that lead to variations in Delta Smelt catch.

Since the general hypothesis is that shallow areas in Suisun Bay are more favorable for Delta Smelt catch than deeper areas (e.g., Moyle et al. 1992; Aasen 1999; Bennett 2005), we also calculated SI_H using Equation 2, but substituting the seabed elevation (a metric for average water depth, see Table 2) for the maximum depth-averaged velocity to evaluate whether increased Delta Smelt catch is simply directed toward shallow regions of Suisun Bay rather than lower velocity areas. However, predictions of SI_H using the seabed elevation were less accurate than the predictions that used the velocity metric. This indicates that although the seabed elevation is correlated to the maximum depth-averaged current speed ($r = -0.771$), lower current speed regions are better predictors of Delta Smelt catch than shallow areas. The less accurate prediction of SI_C using the seabed elevation instead of the maximum depth-averaged current speed is also consistent with seabed elevation ($r = 0.343$) and water depth ($r = -0.248$) being less correlated to SI_C than maximum depth-averaged current speed ($r = -0.533$), as shown in Table 2. In addition, the covariance between the seabed elevation and each of the salinity, Secchi depth, and maximum depth-averaged current speed metrics is higher than the covariance between any of the three selected metrics, indicating that the seabed elevation may be a less suitable metric than the velocity for combining with the salinity and Secchi depth metrics. Since the velocity metric was a better predictor of the historical Delta Smelt catch than water depth, this analysis suggests that lower-velocity areas may be a more important habitat characteristic than shallow water depth for Delta Smelt.

Analysis of Interannual Variability

We investigated the values of SI_H in 2–D throughout Suisun Bay to relate areas historically predicted to be favorable for Delta Smelt catch to environmental conditions which occurred during a drier year in 2010 and a wetter year in 2011. Two key regions for Delta Smelt are Grizzly Bay and Honker Bay, where shallow and flat shoals promote wind-driven resuspension of sediment that increases turbidity (Ruhl et al. 2001). During the fall of the drier year, salinity in Grizzly Bay was above 6 psu (Figure 12A), even though the Secchi depth was less than the 0.5-m value used here as a threshold indicative of historically good conditions for catching Delta Smelt (Figure 12C). The opposite was true for Honker Bay, which had low salinity in 2010 but high Secchi depth (low turbidity). In 2010, favorable salinity and turbidity conditions did not overlap in the regions with low maximum velocity such as Grizzly Bay, Honker Bay, or the

shoals in the middle of Suisun Bay (Figures 12A, 12B, and 12C). In contrast, the wetter year 2011 showed a large portion of Suisun Bay characterized by low salinity (Figure 12B) and low Secchi depth (high turbidity, Figure 12D). The maximum velocity at any given point had much lower interannual variability than salinity and turbidity (Figures 12E and 12F). This results because the main driver behind water velocities in Suisun Bay is tidal forcing (Cheng and Gartner 1984), which when considered over a 4-month period, resulted in velocity metrics that were nearly identical from year to year. Because the velocity metrics are largely invariable on an interannual time scale, potentially favorable regions for Delta Smelt catch can be narrowed to consider the interannual variability in the salinity and turbidity outside of the high-velocity regions. Although the difference in outflow from the Delta between fall 2010 and fall 2011 was large, the differences in outflow in the winter and spring can be much greater than in the fall and some velocity metrics may show more interannual variability and sensitivity to Delta outflow in other seasons (e.g., Monismith et al. 2002).

Comparing the predicted value of SI_H averaged over the fall periods of 2010 and 2011 provides insight into how the variability between wetter and drier years compares to the analysis that focuses on average historical conditions (Figure 13). Because we optimized coefficients in Equation 2 to predict SI_H based on average historical conditions and historical Delta Smelt catch at each station, applying Equation 2 to individual years may not be definitively predictive of exactly where Delta Smelt would be caught in individual years. However, comparing maps of SI_H developed for 2010 and 2011 (Figure 13) to the map developed based on average conditions (Figure 8D) provides insight into how interannual variability in environmental conditions affects predictions of the favorability of a region for Delta Smelt catch.

The overlap of low salinity with low Secchi depth outside of regions of high velocity is a key component to determining locations historically favorable for catching Delta Smelt. This finding that the LSZ needs to overlap with high turbidity is consistent with the present understanding of Delta Smelt catch (Feyrer et al 2007; Sommer and Meija 2013); however, the result that the salinity and turbidity need to overlap in lower-velocity regions has broad implications for determining areas favorable for Delta Smelt catch in the vicinity of Suisun Bay. Two-dimensional spatial maps of SI_H for fall periods following drier (2010) and wetter (2011) years highlight that the area of high SI_H (taken here as greater than 0.5) is much greater when the low salinity and high turbidity overlap outside of high-velocity regions (Figure 13). The overlap of low-salinity and high-turbidity regions is especially important because as Figures 12C and 12D and Ruhl et al. (2001) suggest, the majority of the turbidity in the region around Suisun Bay during low outflow periods—for example, from September through December—is generated through wave resuspension in the shallow areas of Grizzly Bay and Honker Bay. Presumably, if the region of lower salinity retreats eastward, the lower-salinity and higher-turbidity regions may no longer overlap (as was the case in fall 2010), resulting in poorer conditions for Delta Smelt catch than would be predicted based only on the salinity. The FMWT data indicate that 2010 was a poor year for catching Delta Smelt, and 2011 had much higher Delta Smelt catches than 2010, which is consistent with the maps of SI_H (Figure 13) for these 2 years.

Combing Long-term Data Sets and Numerical Model Predictions

A major benefit of a validated numerical model is the ability to sample the model predictions on spatial and temporal scales that would not be possible in a field setting. In this study we used the predicted maximum depth-averaged current speed over a 4-month period to develop the velocity metric. It would not be possible to directly measure this variable at every location within Suisun Bay over a 4-month period. Another benefit of numerical models is that the sub-sampling of model predictions can be done iteratively. If midway through the analysis it is determined that more information is needed, the model predictions could be further sampled to obtain the new information, or the model simulation could be repeated to obtain additional information. This is not possible in a field sampling study that has already been completed. Combining long-term data sets with numerical model predictions could be the

http://dx.doi.org/10.15447/sfews.2016v14iss1art3

focus of further work aiming to better understand historical data collection efforts using metrics that either could not be measured, were too expensive or difficult to observe, or were not thought to be important when the data were being collected. For example, 3–D model predictions could be subsampled at the exact times and locations of tows to better understand the hydrodynamic conditions relating to each specific tow, potentially providing insight into fish catch on a tow-by-tow basis.

The analysis described in this paper could also be performed on other fishes that may have different environmental preferences than Delta Smelt or to different Delta Smelt life stages, to quantitatively assess how environmental factors may have influenced the historical fish catch and to visualize in 2–D the locations predicted to be favorable for catches. The methods presented here can also be transferred to other estuaries with similar long-term fisheries data sets and numerical models. For example, the Virginia Institute of Marine Science trawl survey has tracked trends in seasonal distribution and abundance of finfish and invertebrates in Chesapeake Bay since 1955 (VIMS 2015). Using the approach developed for this study, numerical model predictions from Chesapeake Bay (e.g., Lanerolle et al. 2011; Scully 2013; Feng et al. 2015) could be combined with the trawl survey data to identify the variables most correlated to fish catch for individual species in the Chesapeake Bay.

CONCLUSIONS

A quantitative analysis contributed to a better understanding of the relative historical Delta Smelt catch in the FMWT and Bay Study data sets. The three complexity metrics defined as the percent of the time salinity was less than 6 psu, the maximum depth-averaged current speed, and the Secchi depth at each FMWT station in the vicinity of Suisun Bay were found to be most predictive of historical Delta Smelt catch. The relative ranking of stations for Delta Smelt catch in Suisun Bay across 4 decades could be predicted using these three quantitative metrics of environmental complexity derived from observed data and 3–D model predictions. The high correlation between SI_C and SI_H strongly suggests that the overlap of low salinity and low Secchi depth (high turbidity) in areas with low maximum depth-averaged current speed has historically led to conditions favorable for Delta Smelt catch in Suisun Bay by the FMWT. These results were validated through an independent analysis conducted using the Bay Study Delta Smelt catch data.

Although the salinity and Secchi depth metrics varied significantly between 2010 and 2011, the fall seasonally-averaged velocity metrics were quite similar at any location in Suisun Bay between these 2 years, indicating that interannual variability in the salinity and the Secchi depth metrics are large compared to the interannual variability in the velocity metrics. In 2011, low salinity and low Secchi depth (high turbidity) overlapped in areas with low maximum depth-averaged current speed, but in 2010 the low salinity and low Secchi depth did not overlap in any of the low-velocity regions spanning Grizzly Bay, Honker Bay, or the shallow middle region of Suisun Bay. This co-occurrence of favorable environmental conditions in 2011 but not in 2010 corresponded with the FMWT' reporting much higher Delta Smelt catches in Suisun Bay in 2011 than in 2010.

The predictions of the hydrodynamics from the 3–D numerical model were integral in further understanding spatial variability in the fish catch on scales smaller than the estuary-wide salinity gradient. These results demonstrate that numerical model hindcasts can be combined with long-term data sets to explore environmental conditions at different spatial and temporal scales in order to improve the understanding of observed biological data. Although the current study focused only on the relationship between hydrodynamic complexity and Delta Smelt in the San Francisco Estuary, the method applied here could be extended to other species and areas of interest in this estuary, or to other estuaries.

Baxter et al. (2015) recommend "collaboration among physical and biological modelers, experimental and other scientists, managers, and stakeholders to develop and model management scenarios and strategies that move beyond the current focus on relatively crude distinctions among 'water year types' toward a more integrative ecosystem and landscape-based management approach." This work demonstrates that this type of collaborative approach

can inform future management decisions about the environmental conditions that favor fish catch, and demonstrates the importance of using multiple parameters acting over hourly to inter-annual time-scales to identify the important characteristics of adult Delta Smelt habitat. Substantial effort has been invested in planning for restoration of ecological processes and resources in Suisun Bay and the Delta (BDCP 2014; Resources Agency 2014), and the threatened Delta Smelt has been a particular focus of these efforts. This analysis of the characteristics of habitats that have more consistently yielded Delta Smelt catches in the FMWT, which have been confirmed using the Bay Study, reinforces previous findings that the conditions most likely to support Delta Smelt include low salinity and high turbidity and suggests that the appropriate salinity and turbidity ranges must overlap in areas of relatively low velocity.

ACKNOWLEDGEMENTS

This project was conducted for the U.S. Department of Interior, Bureau of Reclamation, under contract R13PX20111. Renee Hicks (Reclamation) acted as the Contracting Officer and Erwin Van Nieuwenhuyse (Reclamation) acted as the Contracting Officer's Representative for this project. The UnTRIM code was developed by Professor Vincenzo Casulli (University of Trento, Italy). Discussions with Randy Baxter, Lenny Grimaldo, Ken Newman, Lara Mitchell, Leo Polansky, Dave Contreras, and the Estuarine Ecology Team (EET) significantly improved this work. We would also like to thank James Carter (U.S. Geological Survey) and two anonymous reviewers for their comments and suggestions to improve the manuscript.

REFERENCES

Aasen GA. 1999. Juvenile Delta Smelt use of shallow-water and channel habitats in California's Sacramento–San Joaquin Estuary. Calif Fish Game 8(4):161–169.

Armor C, Herrgesell PL. 1985. Distribution and abundance of fishes in the San Francisco Bay estuary between 1980 and 1982. Hydrobiologia 129(1):211–227. doi: *http://dx.doi.org/10.1007/BF00048696*

Bakun A. 2006. Fronts and eddies as key structures in the habitat of marine fish larvae: opportunity, adaptive response and competitive advantage. Sci Mar 70(S2): 105–122. Available from: *http://www.icm.csic.es/scimar/index.php/secId/6/IdArt/194/*

Barletta M, Barletta–Bergan A, Saint–Paul U, Hubold G. 2005. The role of salinity in structuring the fish assemblages in a tropical estuary. J Fish Biol 66:45–72. doi: *http://dx.doi.org/10.1111/j.0022-1112.2005.00582.x*

Baxter R, Weib K, DeLeon S, Fleming K, Orsi J. 1999. Report on the 1980–1995 fish, shrimp, and crab sampling in the San Francisco Estuary, California. Interagency Ecological Program for the San Francisco Bay/Delta Estuary. Technical report no. 63. Sacramento (CA): California Department of Water Resources.

Baxter R, Brown LR, Castillo G, Conrad L, Culberson S, Dekar M, Feyrer F, Hunt T, Jones K, Kirsch J, Mueller–Solger A, Nobriga M, Slater S, Sommer T, Souza K. 2015. An updated conceptual model of Delta Smelt biology: our evolving understanding of an estuarine fish. Interagency Ecological Program for the San Francisco Bay/Delta Estuary. 206 p. Available from: *http://www.water.ca.gov/iep/docs/Delta_Smelt_MAST_Synthesis_Report_January%202015.pdf*

BDCP. 2014. Bay Delta Conservation Plan [draft]. [Internet]. [cited 2015 Oct 30]. Available from: *http://baydeltaconservationplan.com/Home.aspx*

Bennett WA. 2005. Critical assessment of the Delta Smelt population in the San Francisco Estuary, California. San Franc Estuary Watershed Sci 3(2). Available from: *http://escholarship.org/uc/item/0725n5vk* doi: *http://dx.doi.org/10.15447/sfews.2005v3iss2art1*

Bennett WA, Burau JR. 2015. Riders of the storm: selective tidal movements facilitate the spawning migration of the threatened Delta Smelt in the San Francisco Estuary. Estuaries Coasts 38(3):826–835. doi: *http://dx.doi.org/10.1007/s12237-014-9877-3*

http://dx.doi.org/10.15447/sfews.2016v14iss1art3

Bever AJ, MacWilliams M. 2013. Simulating sediment transport processes in San Pablo Bay using coupled hydrodynamic, wave, and sediment transport models. Mar Geol 345:235–253. doi: http://dx.doi.org/10.1016/j.margeo.2013.06.012

Brabrand Å, Faafeng B. 1993. Habitat shift in roach (*Rutilus rutilus*) induced by pikeperch (*Stizostedion lucioperca*) introduction: predation risk versus pelagic behavior. Oecolgia 95(1):38–46. doi: http://dx.doi.org/10.1007/BF00649504

Brown LR, May J. 2006. Variation in spring nearshore resident fish species composition and life histories in the lower Sacramento–San Joaquin watershed and Delta. San Franc Estuary Watershed Sci 4(2). Available from: http://escholarship.org/uc/item/09j597dn doi: http://dx.doi.org/10.15447/sfews.2006v4iss2art1

Brown LR, Baxter R, Castillo G, Conrad L, Culberson S, Erickson G, Feyrer F, Fong S, Gehrts K, Grimaldo L, Herbold B, Kirsch J, Mueller–Solger A, Slater S, Souza K, Van Nieuwenhuyse E. 2014. Synthesis of studies in the fall low-salinity zone of the San Francisco Estuary, September–December 2011. U.S. Geological Survey Scientific Investigations Report 2014–5041. 136 p. Available from: http://www.water.ca.gov/iep/docs/synthesis_sir2014-5041.pdf

[CDFW] California Department of Fish and Wildlife. 2014. Fall Midwater Trawl [Internet]. [cited 2014 Dec 08]. Available from: https://www.dfg.ca.gov/delta/projects.asp?ProjectID=FMWT

[CDWR] California Department of Water Resources. 1995. Estimation of Delta island diversions and return flows. Sacramento (CA): California Department of Water Resources Modeling Support Branch, Division of Planning. Available from: http://www.calwater.ca.gov/Admin_Record/C-032892.pdf

Casulli V. 1999. A semi-implicit numerical method for non-hydrostatic free-surface flows on unstructured grid, In: Numerical modelling of hydrodynamic systems. ESF Workshop, 1999 Jun 21–24; Zaragoza, Spain. p. 175–193.

Casulli V, Walters RA. 2000. An unstructured, three-dimensional model based on the shallow water equations. Int J Numer Meth Fl 32(3):331–348. doi: http://dx.doi.org/10.1002/(SICI)1097-0363(20000215)32:3<331::AID-FLD941>3.0.CO;2-C

Casulli V, Zanolli P. 2002. Semi-implicit numerical modelling of non-hydrostatic free surface flows for environmental problems. Math Comput Model 36(10):1131–1149. Available from: http://dx.doi.org/10.1016/S0895-7177(02)00264-9

Casulli V, Zanolli P. 2005. High resolution methods for multidimensional advection diffusion problems in free-surface hydrodynamics. Ocean Model 10(1–2):137–151. doi: http://dx.doi.org/10.1016/j.ocemod.2004.06.007

Cheng RT, Gartner JW. 1984. Tides, tidal and residual currents in San Francisco Bay, California: results of measurements, 1979–1980. U.S. Geological Survey. Water Resources Investigations Report 84–4339. Available from: https://pubs.er.usgs.gov/publication/wri844339

Elliott M, Dewailly F. 1995. The structure and components of European estuarine fish assemblages. Neth J of Aquatic Ecology 29(3–4):397–417. doi: http://dx.doi.org/10.1007/BF02084239

Essington TE, Hansson S. 2004. Predator-dependent functional responses and interaction strengths in a natural food web. Can J Fish Aquat Sci 61(11):2215–2226. doi: http://dx.doi.org/10.1139/f04-146

Feng Y, Friedrichs MAM, Wilkin J, Tian H, Yang Q, Hofmann EE, Wiggert JD, Hood RR. 2015. Chesapeake Bay nitrogen fluxes derived from a land-estuarine ocean biogeochemical modeling system: model description, evaluation and nitrogen budgets, J Geophy Res 120(8):1666–1695. doi: http://dx.doi.org/10.1002/2015JG002931

Feyrer F, Nobringa M, Sommer T. 2007. Multi-decadal trends for three declining fish species: habitat patterns and mechanisms in the San Francisco Estuary, California, U.S.A. Can J Fish Aquat Sci 136:1393–1405. doi: http://dx.doi.org/10.1139/F07-048

Feyrer F, Newman K, Nobriga M, Sommer T. 2011. Modeling the effects of future outflow on the abiotic habitat of an imperiled estuarine fish. Estuaries Coasts 34(1):120–128. doi: http://dx.doi.org/10.1007/s12237-010-9343-9

Feyrer F, Portz D, Odom D, Newman K, Sommer T, Contreras D, Baxter R, Slater S, Sereno D, Van Niewenhuyse E. 2013. SmeltCam: underwater video codend for trawled nets with an application to the distribution of the imperiled Delta Smelt. PLoS ONE 8(7):e67829. doi: *http://dx.doi.org/10.1371/journal.pone.0067829*

Govoni JJ, Grimes CB. 1992. The surface accumulation of larval fishes by hydrodynamic convergence within the Mississippi River plume front. Cont Shelf Res 12(11):1265–1276. doi: *http://dx.doi.org/10.1016/0278-4343(92)90063-P*

Hood RR, Wang HV, Purcell JE, Houde ED, Harding LW. 1999. Modeling particles and pelagic organisms in Chesapeake Bay: convergent features control plankton distributions. J Geo Res 104:1223–1243. doi: *http://dx.doi.org/10.1029/1998JC900020*

Kai ET, Marsac F. 2010. Influence of mesoscale eddies on spatial structure of top predators' communities in the Mozambique Channel. Prog Oceanogr 86(1–2):214–223. doi: *http://dx.doi.org/10.1016/j.pocean.2010.04.010*

Kimmerer WJ, Gross ES, MacWilliams ML. 2009. Is the response of estuarine nekton to freshwater flow in the San Francisco Estuary explained by variation in habitat volume? Estuaries Coasts 32:375–389. doi: *http://dx.doi.org/10.1007/s12237-008-9124-x*

Kimmerer WJ, MacWilliams ML, Gross ES. 2013. Variation of fish habitat and extent of the low-salinity zone with freshwater flow in the San Francisco Estuary. San Franc Estuary Watershed Sci 11(4). Available from: *https://escholarship.org/uc/item/3pz7x1x8* doi: *http://dx.doi.org/10.15447/sfews.2013v11iss4art1*

Lanerolle LW, Patchen RC, Aikman F. 2011. The second generation Chesapeake Bay operational forecast system (CDOFS2): model development and skill assessment. NOAA Technical Report NOS CS 29. 77 p. Silver Spring (MD): NOAA. Available from: *http://www.nauticalcharts.noaa.gov/csdl/publications/TR_NOS-CS29_FY11_04_Lyon_CBFOS2.pdf*

Lee CH, Dahms HU, Cheng SH, Souissi S, Schmitt FG, Kamur R, Hwang JS. 2010. Predation of *Pseudodiaptomus annandalei* (Copepoda: Calanoida) by the grouper fish fry *Epinephelus coioides* under different hydrodynamic conditions. J Exp Mar Bio Ecol 393(1–2):17–22. doi: *http://dx.doi.org/10.1016/j.jembe.2010.06.005*

MacWilliams ML, Gross ES. 2013. Hydrodynamic simulation of circulation and residence time in Clifton Court Forebay. San Franc Estuary Watershed Sci 11(2). Available from: *http://www.escholarship.org/uc/item/4q82g2bz* doi: *http://dx.doi.org/10.15447/sfews.2013v11iss2art1*

MacWilliams ML, Sing PF, Wu F, Hedgecock N. 2014. Evaluation of the potential salinity impacts resulting from the deepening of the San Francisco Bay to Stockton Navigation Improvement Project In: Proceedings of 33rd PIANC World Congress; 2014 June 1–5; San Francisco, CA. 13 p.

MacWilliams ML, Bever AJ, Gross ES, Ketefian GA, Kimmerer WJ. 2015. Three-dimensional modeling of hydrodynamics and salinity in the San Francisco Estuary: an evaluation of model accuracy, X2, and the low salinity zone. San Franc Estuary Watershed Sci 13(1). Available from: *http://escholarship.org/uc/item/7x65r0tf* doi: *http://dx.doi.org/10.15447/sfews.2015v13iss1art2*

Marshall S, Elliott M. 1998. Environmental Influences on the Fish Assemblage of the Humber Estuary, U.K. Estuarine, Coastal and Shelf Science 46(2):175–184. doi: *http://dx.doi.org/10.1006/ecss.1997.0268*

Menendez M, Piccolo M, Hoffmeyer M. 2012. Short-term variability on mesozooplankton community in a shallow mixed estuary (Bahia Blanca, Argentina): influence of tidal cycles and local winds. Estuar Coast Shelf S 112:11–22. doi: *http://dx.doi.org/10.1016/j.ecss.2011.08.014*

Merz JE, Hamilton S, Bergman PS, Cavallo B. 2011. Spatial perspective for Delta Smelt: a summary of contemporary survey data. Calif Fish Game 97:164–189 Available from: *http://www.genidaqs.net/reports/2011/CA_Fish-Game_97_164-189.pdf*

http://dx.doi.org/10.15447/sfews.2016v14iss1art3

Monismith SG, Kimmerer W, Burau JR, Stacey MT. 2002. Structure and flow-induced variability of the subtidal salinity field in northern San Francisco Bay. J Phys Oceanogr 32:3003–3019. doi: *http://journals.ametsoc.org/doi/abs/10.1175/1520-0485%282002%29032%3C3003%3ASAFIVO%3E2.0.CO%3B2*

Moyle PB, Herbold B, Stevens DE, Miller LW. 1992. Life history and status of Delta Smelt in the Sacramento–San Joaquin Estuary, California. Trans Am Fish Soc 121:67–77. doi: *http://www.tandfonline.com/doi/abs/10.1577/1548-8659%281992%29121%3C0067%3ALHASOD%3E2.3.CO%3B2*

Moyle PB, Bennett WA, Fleenor WE, Lund JR. 2010. Habitat variability and complexity in the upper San Francisco Estuary. San Franc Estuary Watershed Sci 8(3). Available from: *http://escholarship.org/uc/item/0kf0d32x* doi: *http://dx.doi.org/10.15447/sfews.2010v8iss3art1*

Neves L, Mitrano T, Pires T, Pontes T, Hissa H, Gerson F. 2013. Fish composition and assemblage structure in the estuarine mixing zone of a tropical estuary: comparisons between the main channel and an adjacent lagoon. Mar Biol Res 9(7):661–675. doi: *http://dx.doi.org/10.1080/17451000.2013.765575*

Nobriga, M, Feyrer F, Baxter R, and Chotkowski M. 2005. Fish community ecology in an altered river delta: spatial patterns in species composition, life history strategies, and biomass. Estuaries 28:776–785. doi: *http://dx.doi.org/10.1007/BF02732915*

Peterson MS. 2003. A conceptual view of environmental-habitat-production linkages in tidal river estuaries. Rev Fish Sci 11(4):291–313. doi: *http://dx.doi.org/10.1080/10641260390255844*

[Resources Agency] State of California, The Resources Agency. 2012. Fish Restoration Program Agreement (FRPA) implementation strategy. 117 p. Available from: *http://www.water.ca.gov/environmentalservices/docs/Implementation_Strategy_Final_for_printing_031612.pdf*

[Resources Agency] State of California, The Resources Agency. 2014. Conservation strategy for restoration of the Sacramento–San Joaquin Delta, Sacramento Valley and San Joaquin Valley regions. 255 p. Available from: *https://nrm.dfg.ca.gov/FileHandler.ashx?DocumentID=31232&inline*

Ruhl CA, Schoellhamer DH, Stumpf RP, Lindsay CL. 2001. Combined use of remote sensing and continuous monitoring to analyze the variability of suspended–sediment concentrations in San Francisco Bay, California. Estuar Coast Shelf Sci 53:801–812. doi: *http://dx.doi.org/doi:10.1006/ecss.2000.0730*

Scully ME. 2013. Physical controls on hypoxia in Chesapeake Bay: a numerical modeling study. J Geophys Res 118(3):1239–1256. doi: *http://dx.doi.org/10.1002/jgrc.20138*

Sommer T, Armor C, Baxter R, Bruer R, Brown L, Chotkowski M, Culberson S, Feyrer F, Gingras M, Herbold B, Kimmerer W, Mueller–Solger A, Nobringa M, Souza K. 2007. The collapse of pelagic fishes in the upper San Francisco Estuary. Fisheries 32(6):270–277. doi: *http://dx.doi.org/10.1577/1548-8446(2007)32[270:TCOPFI]2.0.CO;2*

Sommer T, Mejia F. 2013. A place to call home: a synthesis of Delta Smelt habitat in the upper San Francisco Estuary. San Franc Estuary Watershed Sci 11(2). Available from: *http://escholarship.org/uc/item/32c8t244* doi: *http://dx.doi.org/10.15447/sfews.2013v11iss2art4*

Stevens DE, Miller LW. 1983. Effects of river flow on abundance of young Chinook Salmon, American Shad, Longfin Smelt, and Delta Smelt in the Sacramento–San Joaquin river system. N Am J Fish Manage 3(4):425–437. doi: *http://www.tandfonline.com/doi/abs/10.1577/1548-8659%281983%293%3C425%3AEORFOA%3E2.0.CO%3B2*

Thiel R, Sepúlveda A, Kafemann R, Nellen W. 1995. Environmental factors as forces structuring the fish community of the Elbe Estuary. J Fish Biol 46(1):47–69. doi: *http://dx.doi.org/10.1111/j.1095-8649.1995.tb05946.x*

Trenkel VM, Huse G, MacKenzie BR, Alvarez P, Arrizabalaga H, Castonguay M, Goñi N, Grégoire F, Hátún H, Janse T, Jacobsen JA, Lehodey P, Lutcavage M, Mariani P, Melvin GD, Nielsen JD, Nøttestad L, Óskarson JG, Payne MR, Richardson DE, Senina I, Speirs DC. 2014. Comparative ecology of widely distributed pelagic fish species in the North Atlantic: implications for modelling climate and fisheries impacts. Prog Oceanogr 129:219–243. doi: *http://dx.doi.org/10.1016/j.pocean.2014.04.030*

Umlauf L, Burchard H. 2003. A generic length–scale equation for geophysical turbulence models. J Mar Res 61:235–265. doi: *http://dx.doi.org/10.1357/002224003322005087*

[VIMS] Virginia Institute of Marine Science. 2015. Juvenile fish and blue crab trawl survey [Internet]. [cited 2015 Nov 17]. Available from: *http://www.vims.edu/research/departments/fisheries/programs/juvenile_surveys/index.php*

Walters CJ, Juanes F. 1993. Recruitment limitation as a consequence of natural selection for use of restricted feeding habitats and predation risk taking be juvenile fishes. Can J Fish Aquat Sci 50:2058–2070. doi: *http://dx.doi.org/10.1139/f93-229*

Warner JC, Sherwood CS, Arango HG, Signell RP. 2005. Performance of four turbulence closure models implemented using a generic length scale method. Ocean Model 8:81–113. doi: *http://dx.doi.org/10.1016/j.ocemod.2003.12.003*

http://dx.doi.org/10.15447/sfews.2016v14iss1art3